YITP-12-16, IPM/P-2012/011

Local Features with Large Spiky non-Gaussianities during Inflation

Ali Akbar Abolhasani[1],* Hassan Firouzjahi[1],† Shahram Khosravi[2],‡ and Misao Sasaki[3]§
[1] *School of Physics, Institute for Research in Fundamental Sciences (IPM), P. O. Box 19395-5531, Tehran, Iran*
[2] *Physics Department, Faculty of Science, Tarbiat Moallem University, Tehran, Iran,*
and School of Astronomy, Institute for Research in Fundamental Sciences(IPM), Tehran, Iran. and
[3] *Yukawa Institute for theoretical Physics, Kyoto University, Kyoto 606-8502, Japan*
(Dated: March 2, 2013)

arXiv:1204.3722v1 [astro-ph.CO] 17 Apr 2012

We provide a dynamical mechanism to generate localized features during inflation. The local feature is due to a sharp waterfall phase transition which is coupled to the inflaton field. The key effect is the contributions of waterfall quantum fluctuations which induce a sharp peak on the curvature perturbation which can be as large as the background curvature perturbation from inflaton field. Due to non-Gaussian nature of waterfall quantum fluctuations a large spike non-Gaussianity is produced which is narrowly peaked at modes which leave the Hubble radius at the time of phase transition. The large localized peaks in power spectrum and bispectrum can have interesting consequences on CMB anisotropies.

PACS numbers:

I. INTRODUCTION

Simplest inflationary scenarios predict almost scale invariant, almost Gaussian and almost adiabatic perturbations and the observed cosmic microwave background (CMB) anisotropies are in very good agreements with these predictions [1]. However, with higher precision data expected to come from near future cosmological observations such as PLANCK, one hopes that some deviations from the predictions of single-field inflation may be observed. In particular a detection of non-Gaussianity would exclude a large class of inflationary scenarios.

There have been many attempts in the literature to generalize local features during inflation which may have non-trivial predictions on the power spectrum and bispectrum [2–13]. This is partly motivated from glitches in the CMB angular power spectrum at $\ell \sim 20 - 40$. These local features may originate from models of high energy physics, particle creation or field annihilation during inflation [14–24].

In many of these models local features are generated by temporal violations of slow-roll conditions during inflation. However, many of them are based on rather ad hoc mechanisms to violate slow-roll conditions. In this work, we provide a dynamical mechanism to generate local features in the power spectrum and bispectrum. The model consists of a simple chaotic inflation potential, $m^2\phi^2/2$, coupled to a heavy field χ. After ϕ reaches a critical value $\phi = \phi_c (\gg M_P)$, χ becomes tachyonic and a rapid waterfall phase transition takes place. In this sense the model is similar to hybrid inflation [25, 26]. However, the key difference is that the potential is not vacuum dominated but the chaotic type inflaton potential is the main driving source of inflation. Furthermore, inflation continues even after the waterfall phase transition.

In this model, inflation may be divided into three stages. At the first stage $\phi > \phi_c$, inflation proceeds as in chaotic inflation. The second stage at which $\phi \lesssim \phi_c$ is fairly short, of the order of the Hubble time, and χ becomes tachyonic and a waterfall phase transition takes place where χ settles to its global minimum. This causes a small change in the inflaton effective mass, $m^2 \to m_+^2 = m^2(1 + C)$ where $C << 1$. Then the third stage proceeds as in chaotic inflation again. In order to bring the local feature into the observable windon of CMB, we demand that the phase transition takes place $50 - 60$ e-folds before the end of inflation.

The key point in our analysis is the evaluation of the waterfall quantum fluctuations and its contribution to the curvature perturbation on uniform density slices ζ [27]. For studies of the waterfall contribution to ζ, in the context of hybrid inflation, see [28–49].

Due to the sharpness of the waterfall phase transition, the waterfall contribution in ζ is narrowly localized around

---

*Electronic address: abolhasani-AT-mail.ipm.ir
†Electronic address: firouz-AT-mail.ipm.ir
‡Electronic address: khosravi-AT-mail.ipm.ir
§Electronic address: misao-AT-yukawa.kyoto-u.ac.jp

the modes which leave the horizon at the time of waterfall transition. Furthermore, due to the intrinsically non-Gaussian nature of the waterfall contribution, which is in the form of $\zeta \sim \delta\chi^2$, a large spiky bispectrum is generated. We emphasize that this is a local dynamical effect intrinsic to the waterfall quantum fluctuations which are absent in other models, hence is an observationally testable feature genuinely specific to our model.

The rest of paper is organized as follows. In Section II we present our model and basic setup. In Section III we calculate ζ using the δN formalism. In Section V we calculate the dynamical and intrinsic non-Gaussianities in our scenario followed by conclusion and discussions in Section VI. Technical details about the power spectrum of the waterfall quantum fluctuations and higher order δN perturbations are deferred to appendices.

II. THE MODEL

In this section we present our setup in modeling local features during inflation. In our picture, we consider the simplest inflationary model, the chaotic potential $m^2\phi^2/2$, where we assume the mass of inflaton undergoes a sudden dynamical change at $\phi = \phi_c$. We would like to see how a sudden small change in the inflaton mass can be modeled in a consistent dynamical way and then look for its observational consequences in CMB. One of the best known dynamical mechanism for inducing local feature during inflation is the idea of waterfall phase transition. For this purpose, we consider the following setup:

$$V = \frac{m^2}{2}\phi^2 + \frac{\lambda}{4}\left(\chi^2 - \frac{M^2}{\lambda}\right)^2 + \frac{g^2}{2}\phi^2\chi^2 \,, \tag{2.1}$$

where ϕ is the inflaton field and χ is the waterfall field. Formally potential (2.1) is identical to hybrid inflation [25, 26]. However, as we mentioned above, in our picture inflation is mainly driven by the field ϕ so in our picture effectively inflation proceeds as in chaotic model with potential $V \simeq m_{eff}^2\phi^2/2$ with some effective mass m_{eff} which undergoes a small but abrupt change at $\phi = \phi_c$. The waterfall field χ is employed to induce this change in mass.

In this model, like in chaotic inflation, inflation starts at $\phi = \phi_i \gg M_P$, with $M_P^2 = (8\pi G)^{-1}$ for G being the Newton constant, so one can obtain 60 e-folds or more to solve the horizon and flatness problems. The waterfall field is very heavy during the first stage of inflation so it remains at its instantaneous minimum $\chi = 0$. Once the inflaton field reaches the critical value $\phi = \phi_c \equiv M/g$, the waterfall field χ becomes tachyonic and quickly rolls down to its global minimum $\chi_{min}^2 = M^2/\lambda$. The final stage of inflation after $\phi > \phi_c$ proceeds as in chaotic inflation again but with the effective mass of the inflaton, m_+, given by

$$m_+^2 = m^2 + g^2\langle\chi^2\rangle = m^2\left(1 + C\right) \tag{2.2}$$

where

$$C \equiv \frac{g^2M^2}{\lambda m^2} \,. \tag{2.3}$$

In our model, we assume the change in inflaton mass is small, $C \ll 1$. In order to bring this local feature into the observable scale, we assume that the short waterfall stage which lasts for about an e-fold or so begins at around 55 e-folds before the end of inflation.

It is instructive to look into different contributions to the potential before the phase transition where $V = m^2\phi^2/2 + M^4/4\lambda$. We have $V(\phi_c) = m^2\phi_c^2/2(1 + C/2)$. Having $C \ll 1$ in our model corresponds to the assumption that the inflationary potential is dominated by the $m^2\phi^2/2$ term. This is in contrast to the standard hybrid inflation where the potential is vacuum dominated corresponding to $C \gg 1$.

Before we proceed further we pause to compare our scenario to the one studied in [6] where the potential is still given by Eq. (2.1). However, in [6] they are interested in the limit where $C \gtrsim 1$ so inflation is mildly vacuum dominated. Hence their model is effectively a single field model where the waterfall quantum fluctuations can be neglected. In contrast, in the present paper we pay careful attention to the dynamics of the waterfall phase transition and calculate rigorously the curvature perturbations induced from the waterfall quantum fluctuations. For this to happen, we require $\phi_c \gtrsim 10M_P$.

As usual the cosmological background is given by

$$ds^2 = -dt^2 + a(t)^2 d\mathbf{x}^2 \,, \tag{2.4}$$

where $a(t)$ is the scale factor. It is more convenient to change the clock from the cosmic time t to the number of e-folds N via $dN = Hdt$ where $H = \dot{a}/a$ is the Hubble expansion rate. Denoting the time when the waterfall phase transition takes place by N_c, we further define $n \equiv N - N_c$. Hence $n < 0$ for the period before the phase transition and $n > 0$ after the transition. We denote the end of the waterfall transition when χ has settled down to its global minimum by $n = n_f$. With this notation, inflation in our model has the three stages: (a): $n < 0$, (b): $0 \leq n \leq n_f$ and (c): $n_f < n < N_e - N_c$ where N_e is the time when the inflation ends. We set $N_e - N_c \sim 55$ so that the waterfall transition falls into the observable range.

We are interested in the limit where the waterfall phase transition is fairly sharp, corresponding to $n_f \lesssim 1$ so the waterfall transition and symmetry breaking completion takes place in an e-fold or so. The key ingredient in our analysis is the dynamics of the waterfall quantum fluctuations during this short period and the curvature perturbations induced from them. To investigate this we will use the δN formalism [27, 50–52].

As mentioned before, we assume that the waterfall field is very heavy so it stays at $\chi = 0$ and $\chi = \chi_{min}$ during the first and third stages. It is useful to introduce the dimensionless parameters α and β by

$$\alpha \equiv \frac{m^2}{H^2} \simeq \frac{6M_P^2}{\phi^2} \simeq \frac{6g^2M_P^2}{M^2} \quad , \quad \beta \equiv \frac{M^2}{H^2} \simeq \frac{6M^2M_P^2}{m^2\phi^2} \simeq \frac{6g^2M_P^2}{m^2} \, , \tag{2.5}$$

where in the last approximate equalities in both expressions it is assumed that $\phi \simeq \phi_c$. The assumption that the slow-roll conditions hold during the first and third inflationary stages requires $\alpha \ll 1$. Demanding that $\beta \gg 1$ for the waterfall field to be heavy, we require $g^2 \gg m^2/M_P^2$. On the other hand, from the COBE normalization we have $m/M_P \sim 10^{-6}$ so $g^2 \gg 10^{-12}$. Furthermore, we assume the onset of the phase transition and the time of sudden change in the inflaton mass to occur about 55 e-folds before the end of inflation so that it falls within the CMB observational window. In order for inflation to proceed long enough after the phase transition as in the standard chaotic inflation we require $\phi_c \gtrsim 10M_P$ so $g^2 \lesssim 10^{-2}M^2/M_P^2$. Combining this with $g^2 \gg m^2/M_P^2$ we get $m^2 \ll 10^{-2}M^2$ or $M \gg 10^{-5}M_P$. Finally, from the definition of C we conclude that $g^2/\lambda \ll 10^{-2}C$. For example if we take $C \sim 10^{-2}$, we have $g^2/\lambda \ll 10^{-4}$ and $\lambda = C^{-1}g^2M^2/m^2 \sim 10^2g^2M^2/m^2 \gg 10^4g^2 \gg 10^{-8}$.

A. Inflaton dynamics

As mentioned above during the first and second stage, inflation proceeds as in chaotic inflation with the potential,

$$V^-(\phi) \;=\; \frac{1}{2}m^2\phi^2 + \frac{M^4}{4\lambda}. \tag{2.6}$$

During the short second stage χ grows until the self-interaction term $\lambda\chi^4$ becomes important. Then the self-interaction induces a large mass and χ settles down to its local minimum. We denote this time by n_f. After that, the waterfall field starts rolling across the valley determined by $\partial_\chi V(\phi, \chi) = 0$. This gives

$$\chi^2 = \chi^2_{min} \equiv \frac{M^2}{\lambda} - \frac{g^2}{\lambda}\phi^2. \tag{2.7}$$

As seen from the above equation the local value of χ at the third stage is dictated by the value of the inflaton field. Accordingly, during the third stage, the inflaton field experiences an effective potential given by

$$V^+_{eff}(\phi) = V(\phi, \chi(\phi)) = \frac{1}{2}m^2(1+C)\phi^2 - \frac{g^4}{4\lambda}\phi^4. \tag{2.8}$$

Solving the slow-roll equations of motion for ϕ, we obtain, for the first and second stages,

$$-4M_P^2(N - N_c) = -4M_P^2\, n \;=\phi(n)^2 - \phi_c^2\left[1 - C\ln\left(\frac{\phi}{\phi_c}\right)\right] , \tag{2.9}$$

whereas for the third stage,

$$\begin{aligned} 8M_P^2(N_e - N) \;&=\; -\phi_e^2 + \phi(N)^2 + \frac{1+C}{C}\;\phi_c^2\,\ln\left[\frac{1 - \dfrac{C}{1+C}\dfrac{\phi_e^2}{\phi_c^2}}{1 - \dfrac{C}{1+C}\dfrac{\phi^2}{\phi_c^2}}\right] & (2.10)\\ &=\; 2\phi^2(N) - 2\phi_e^2 + \frac{C}{2}\,\frac{\phi^4(N) - \phi_e^4}{\phi_c^2} + O(C^2)\,. & (2.11)\end{aligned}$$

As usual inflation ends at $\phi = \phi_e$ where the slow-roll conditions $\epsilon, \eta \ll 1$ are terminated corresponding to $\phi_e = \sqrt{2}M_P$. The slow-roll parameters are defined via

$$\epsilon \equiv \frac{M_P^2}{2}\left(\frac{V_\phi}{V}\right)^2 \quad , \quad \eta \equiv M_P^2 \frac{V_{\phi\phi}}{V} \,. \tag{2.12}$$

In the present case, around the epoch of the phase transition, the slow-roll parameters are approximately expressed in terms of the parameter α as

$$\epsilon \simeq \eta \simeq \frac{\alpha}{3} \,. \tag{2.13}$$

B. Waterfall Field Dynamics

In this section we study the dynamics of the waterfall quantum fluctuations. One key point in our model, similar to hybrid inflation, is that before the waterfall transition χ is very heavy so that it firmly stays at its local minimum $\chi = 0$ and classically there is no background evolution of the waterfall field. Following the prescription in [29] we assume that for each horizon-size patch one would observe $\delta\chi^2$ as a homogeneous classical background which varies smoothly over scales larger than the horizon scale. Thus on a given, sufficiently large scale, say the comoving scale of the present Hubble horizon size, one can calculate the mean value $\langle \delta\chi^2(n) \rangle$ and the fluctuation,

$$\Delta\chi^2(n, \mathbf{x}) \equiv \delta\chi^2(n, \mathbf{x}) - \langle \delta\chi^2(n) \rangle \,, \tag{2.14}$$

where $\langle \delta\chi^2(n) \rangle$ determines the homogeneous background while $\Delta\chi^2(n, \mathbf{x})$ gives rise to the curvature perturbations on super-horizon scales.

With this understanding we now look into the dynamics of the background waterfall field and its quantum fluctuations in some details. The background waterfall dynamics is governed by

$$\chi'' + 3\chi' + \left(-\beta + g^2\frac{\phi^2}{H^2} + 3\lambda\frac{\chi^2}{H^2}\right)\chi = 0 \,, \tag{2.15}$$

where here and below the prime denotes a derivative with respect to n. Neglecting the self-interaction term $\lambda\frac{\chi^2}{H^2}$ during the second stage when the transition proceeds, an approximate solution for the background waterfall field is given by [29]

$$\chi(n) \simeq \chi(n=0)\, \exp\left[\frac{2}{3}\epsilon_\chi n^{3/2}\right] \,, \tag{2.16}$$

where

$$\epsilon_\chi \simeq \sqrt{\frac{2}{3}\alpha\beta} \,. \tag{2.17}$$

Here it is worth noting the relations among the model parameters. Our model has four parameters: M, m, g and λ. On the other hand, we have introduced six non-dimensional parameters: α, β, ϵ, η, ϵ_χ and C. Some of these are functions of time, but at leading order in the slow-roll approximation, we may consider them as constants. Then as a convenient set of independent parameters, we may choose ϵ, C, ϵ_χ and λ. Then we have

$$\begin{gathered} \alpha = 3\epsilon \,, \quad \beta = \frac{\epsilon_\chi^2}{2\epsilon} \,, \quad \eta = \epsilon \,, \quad g^2 = \frac{6\lambda\epsilon^2 C}{\epsilon_\chi^2} \\ M^2 \simeq \frac{12\lambda\epsilon C}{\epsilon_\chi^2}M_P^2 \,, \quad m^2 \simeq \frac{72\lambda\epsilon^3 C}{\epsilon_\chi^4}M_P^2 \,. \end{gathered} \tag{2.18}$$

The dynamics of the waterfall field quantum fluctuations in Fourier space, neglecting the self-interaction term, is governed by

$$\delta\chi''_{\mathbf{k}} + 3\delta\chi'_{\mathbf{k}} + \left(\frac{k^2}{a^2H^2} - \beta + g^2\frac{\phi^2}{H^2}\right)\delta\chi_{\mathbf{k}} = 0 \,, \tag{2.19}$$

where

$$\delta\chi_{\mathbf{k}} = \int \frac{d^3x}{(2\pi)^{3/2}}\,\delta\chi(\mathbf{x})e^{-i\mathbf{k}\cdot\mathbf{x}} = a_{\mathbf{k}}\chi_k(n) + a^\dagger_{-\mathbf{k}}\overline{\chi_k(n)}\,. \tag{2.20}$$

Here $a_{\mathbf{k}}$ and $a^\dagger_{\mathbf{k}}$ are the annihilation and creation operators, respectively, with respect to a suitably chosen vacuum and $\chi_k(n)$ is the positive frequency function. Plugging the background value of ϕ given by Eq. (2.9) into Eq. (2.19) results in

$$\delta\chi''_{\mathbf{k}} + 3\delta\chi'_{\mathbf{k}} + \left(\frac{k^2}{k_c^2}e^{-2n} - \epsilon_\chi^2 n\right)\delta\chi_{\mathbf{k}} = 0\,, \tag{2.21}$$

where k_c is the comoving momentum of the mode which exits the horizon at the time of waterfall phase transition: $k_c = Ha(n=0)$. As seen from Eq. (2.21), $\epsilon_\chi H^2$ measures the effective tachyonic mass of the waterfall field when the tachyonic instability develops. The assumption that the waterfall phase transition is sharp requires that $\epsilon_\chi \gg 1$. The normalization of $\chi_{\mathbf{k}}$ is determined by the canonical commutation relation, which gives

$$\delta\chi_{\mathbf{k}}\overline{\delta\chi}'_{\mathbf{k}} - \overline{\delta\chi}_{\mathbf{k}}\delta\chi'_{\mathbf{k}} = \frac{iH^2}{k_c^3 e^{3n}}\,. \tag{2.22}$$

For large and negative n, Eq. (2.21) can be solved by the WKB approximation by setting $\delta\chi_{\mathbf{k}} \propto \exp[S_0 + S_1 + \cdots]$. Taking account of the normalization condition (2.22) and choosing the standard Minkowski positive frequency in the limit $n \to -\infty$, the result to first order in the WKB approximation is [32]

$$\delta\chi_k(n) = \frac{H}{\sqrt{2k_c^3}}\frac{e^{-3n/2}}{\left((k/k_c)^2e^{-2n} - \epsilon_\chi^2 n\right)^{1/4}}\exp\left[-i\int^n \left((k/k_c)^2e^{-2n'} - \epsilon_\chi^2 n'\right)^{1/2}dn'\right]\,. \tag{2.23}$$

After waterfall phase transition, $n > 0$, some (low k) quanta of the waterfall field become tachyonic and behave like classical random fields [31]. In particular there are modes which become tachyonic even before horizon crossing. In order to find the dynamics of the waterfall quantum fluctuations, it is convenient to divide the modes into large and small modes which we denote below by the subscripts L and S, respectively. Large modes are those which exit the horizon before the time of the phase transition $n = 0$ and small modes are those which are sub-horizon at $n = 0$.

The large modes cross the horizon sometime before the waterfall transition and after horizon crossing their profile decays like $\propto e^{-3n/2}$ as seen from Eq. (2.23). At the time of transition, $n = 0$, the WKB approximation fails, but apart from a factor of order unity, the amplitude at $n = 0$ is approximately given by

$$|\delta\chi^L_{\mathbf{k}}(n=0)| \simeq \frac{H}{\sqrt{2\epsilon_\chi k_c^3}}\,. \tag{2.24}$$

After the transition, $n > 0$, these modes follow the same equation as the classical trajectory does. So by using Eq. (2.16) one has

$$|\delta\chi^L_{\mathbf{k}}(n>0)| \simeq \frac{H}{\sqrt{2\epsilon_\chi k_c^3}}\exp\left(\frac{2}{3}\epsilon_\chi n^{3/2}\right)\,. \tag{2.25}$$

The situation for the small modes is a bit complicated and requires careful considerations. As mentioned above the effective tachyonic mass of $\delta\chi_{\mathbf{k}}$ is of the order of $\epsilon_\chi H \gg H$. As a result some modes become tachyonic even before horizon crossing. For modes which become tachyonic the spatial gradient term becomes negligible compared to the tachyonic mass and the evolution of $\delta\chi_{\mathbf{k}}$ becomes identical to that of the background solution. So for each mode it is important to find the time when it becomes tachyonic. Denoting the time when the mode k becomes tachyonic by $n_t(k)$, from Eq. (2.21) one has

$$n_t(k)e^{2n_t(k)} = \left(\frac{k}{\epsilon_\chi k_c}\right)^2\,. \tag{2.26}$$

Later on we shall call this time the "classicalization" time. The solution of the above algebraic equation are known to be given by the Lambert W function $W(z)$,

$$n_t(k) = \frac{1}{2}W(z); \quad z = 2\left(\frac{k}{\epsilon_\chi k_c}\right)^2\,, \tag{2.27}$$

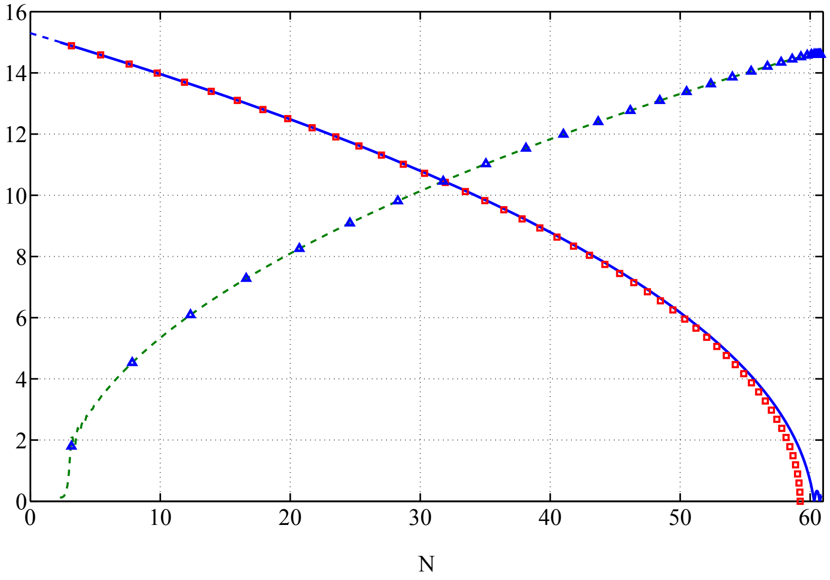

FIG. 1: Dynamics of the inflaton and waterfall fields (smoothed over a horizon-size patch). The solid blue line (the red squares) shows the numerical solution (analytical estimate in Eq. (2.10)) for inflaton field . The short dashed blue line for small N shows the dynamics of the inflaton field before the transition point. As one can see in this figure the inflaton dynamics before and after transition are connected smoothly. The dashed green line (the blue triangles) shows our numerical (analytical estimate) results for the dynamics of the waterfall field in a smoothing patch. In order to visualize this figure better the waterfall field amplitude is multiplied by a factor 2×10^3. The model parameters are $m = 6 \times 10^{-6} M_P$, $g^2 = 3 \times 10^{-8}$, $\lambda = 0.14$ and $\phi_c = M/g = 15 M_P$, which give $C = .15$ and $\epsilon_\chi = 20$.

but we only need an approximate solution for $n_t(k)$ since $n_t(k) \lesssim 1$ for the parameters of our interest.

One can use the WKB solution Eq. (2.23) until $n = n_t(k)$, which gives

$$\delta\chi^S_{\mathbf{k}}(n) = \frac{H}{\sqrt{2k}\, k_c} e^{-n} \, ; \quad n < n_t(k) \, . \tag{2.28}$$

After $n = n_t(k)$ this mode evolves as the classical background solution, Eq. (2.16). By matching the solution with the classical trajectory at $n = n_t(k)$, for $n > n_t(k)$ one approximately has

$$\delta\chi^S_{\mathbf{k}}(n) = \frac{H}{\sqrt{2k}\, k_c} e^{-n_t} \exp\left[\frac{2}{3}\epsilon_\chi (n^{3/2} - n_t^{3/2})\right] \; ; \quad n > n_t(k) \, . \tag{2.29}$$

Here it is convenient to project $\delta\chi^S_k(n)$ at time of the onset of waterfall $n = 0$ as if all the modes were tachyonic at $n > 0$, as viewed in [29, 32]. This gives

$$\delta\chi^S_{\mathbf{k}}(0) = \frac{H}{\sqrt{2k}\, k_c} \exp\left[-n_t(k) - \frac{2}{3}\, \epsilon_\chi n_t^{3/2}(k)\right] \, . \tag{2.30}$$

Because of the exponential growth of the waterfall field quantum fluctuations after the transition, the expectation value $\langle \delta\chi^2 \rangle$ becomes non-negligible and its rms value soon starts to behave as a classical field [29] $\chi = \sqrt{\langle \delta\chi^2 \rangle}$. As a result $\langle \delta\chi^2 \rangle$ is observed as a classical background for an observer within each Hubble horizon region [29, 31, 32]. Therefore it is necessary to calculate $\langle \delta\chi^2 \rangle$ given in terms of its power spectrum $\mathcal{P}_{\delta\chi}$ as

$$\langle \delta\chi^2 \rangle = \int \frac{d^3k}{(2\pi)^3} |\delta\chi_{\mathbf{k}}|^2 = \int \frac{d^3k}{(2\pi)^3} P_\chi(k) = \int \frac{dk}{k} \mathcal{P}_{\delta\chi}(k) \, , \tag{2.31}$$

where the power spectrum is defined by

$$\langle \delta\chi_{\mathbf{k}} \delta\chi_{\mathbf{q}} \rangle \equiv (2\pi)^3 \delta^3(\mathbf{k} + \mathbf{q}) P_\chi(k) \, , \quad \mathcal{P}_{\delta\chi} \equiv \frac{k^3}{2\pi^2} P_\chi(k) \, . \tag{2.32}$$

By using Eqs. (2.25) and (2.29) one can read off the power spectrum of the waterfall quantum fluctuations at $n = 0$ as

$$\mathcal{P}_{\delta\chi}(k;0) = \begin{cases} \dfrac{H^2}{4\pi^2\epsilon_\chi}\left(\dfrac{k}{k_c}\right)^3 ; & k < k_c\,, \\ \dfrac{H^2\epsilon_\chi^2}{4\pi^2}\, n_t(k)\exp\Big[-\tfrac{4}{3}\epsilon_\chi n_t^{3/2}(k)\Big] ; & k > k_c\,. \end{cases} \tag{2.33}$$

The details of the analysis to calculate $\langle\delta\chi^2\rangle$ is given in Appendix A where it is found that $\langle\delta\chi^2\rangle$ is dominated by the small scale modes,

$$\langle\delta\chi^2(0)\rangle \simeq \langle\delta\chi^2(0)\rangle_S \simeq \frac{3\epsilon_\chi^{4/3}H^2}{16\pi^2}\,. \tag{2.34}$$

As seen from Eq. (2.33), there is a sharp peak in the spectrum of waterfall quantum fluctuations. In order to estimate the width of the peak, we expand the above spectrum around its peak. Solving $\partial\mathcal{P}_{\delta\chi}/\partial n_t = 0$, the peak position is found as

$$n_t(k_{max}) = \left(\frac{1}{2\epsilon_\chi}\right)^{2/3}\,. \tag{2.35}$$

Expanding the spectrum around this momentum, one finds

$$\mathcal{P}_{\delta\chi}(k;0) \simeq \frac{H^2\epsilon_\chi^2}{4\pi^2}\left(\frac{1}{2e\,\epsilon_\chi}\right)^{2/3}\exp\left[-\frac{(n_t(k)-n_t(k_{max}))^2}{2\sigma_{n_t}^2}\right]\,, \tag{2.36}$$

with

$$\sigma_{n_t} = \sqrt{\frac{2}{3}}\left(\frac{1}{2\epsilon_\chi}\right)^{2/3} = \sqrt{\frac{2}{3}}n_t(k_{max})\,. \tag{2.37}$$

But we are interested in the width of spectrum in momentum space, $\sigma_*(k)$. By using Eq. (2.26) it is readily found as

$$\begin{aligned} \sigma_*(k) &= \left(1+\frac{1}{2n_t(k)}\right)\sigma_{n_t}k_{max} && (2.38)\\ &\simeq \left(\sqrt{\frac{1}{6}}+\mathcal{O}(\epsilon_\chi^{-2/3})\right)k_{max} \simeq 0.4k_{max}\,. && (2.39)\end{aligned}$$

This indicates that the width of the waterfall power spectrum is independent of the sharpness of the phase transition for large ϵ_χ, which we verified also numerically.

III. δN FORMALISM AND CURVATURE PERTURBATIONS

In this section, using the δN formalism [50], [51], [27] and [52], we calculate the curvature perturbations. In order to use the δN formalism properly we trace back the number of e-folds from the end of inflation until the time of horizon crossing for each mode. To avoid confusion we denote the number of e-folds counted *backward* in time from the end of inflation by $\mathcal{N}$, that is, $\mathcal{N} \equiv N_e - N$. Our strategy is to express $\mathcal{N}$ in terms of the fields $\phi(n)$ and $\chi^2(n)$ (smoothed on every Hubble patch).

For those modes which exit the horizon after the waterfall transition, by using Eq. (2.11), one can easily find the curvature perturbation on comoving slices, $\mathcal{R}_c$, as

$$\mathcal{R}_c = \delta\mathcal{N} = \left(1+\frac{C}{2}\frac{\phi^2}{\phi_c^2}\right)\frac{\phi\,\delta\phi}{2M_P^2}\,, \tag{3.1}$$

where $\delta\phi$ is to be evaluated on flat hypersurface as usual. Finding the curvature perturbation for those modes which exit the horizon before and during transition needs careful calculations. Here, we follow the same step as in [31] for these modes.

Here it is worth mentioning that the duration of the waterfall stage is sensitive to the classical value of the waterfall field on every smoothing patch. As discussed before, because of the large tachyonic mass of the waterfall field there are modes whose spatial gradient can be neglected and which behave classically already before their scales cross the horizon, and hence affect the classical trajectory. Noting that the formula $\mathcal{R}_c = \delta\mathcal{N}$ is valid on scales over which small scale inhomogeneities can be smoothed out with a negligible influence on the geometry, we take the smoothing scale to be slightly larger than the comoving scale corresponding to the wavelength of the last mode which becomes tachyonic.

As we discussed before, during the third inflationary stage (after completion of the phase transition) inflation proceeds in the form of chaotic inflation with a slight change in the effective mass of the inflaton. So the end of inflation is determined by the value of ϕ alone as

$$\phi = \phi_e \approx \sqrt{2}\, M_P \,. \tag{3.2}$$

From this point up to the time of the end of the waterfall transition, $\mathcal{N}$ is given by Eq. (2.11),

$$\mathcal{N} = \frac{1}{4M_P^2}\left[\phi^2 - \phi_e^2 + \frac{C}{4}\frac{\phi^4 - \phi_e^4}{\phi_c^2}\right]; \quad \mathcal{N} \le \mathcal{N}_f \,, \tag{3.3}$$

where $\mathcal{N}_f$ is the value of $\mathcal{N}$ at the end of the waterfall transition. Here, for simplicity we consider that at the end of transition χ is very close to its local instantaneous minimum so χ^2 at $\mathcal{N} = \mathcal{N}_f$ is

$$\chi^2(n_f) = \chi^2_{min}(n_f) \simeq \frac{M^2}{\lambda} - \frac{g^2}{\lambda}\phi_f^2. \tag{3.4}$$

One can obtain $\mathcal{N}_f$ in terms of the number of e-folds from the critical epoch $\phi = \phi_c$ to the end of waterfall transition, n_f, as

$$\mathcal{N}_f(n_f) = \frac{1}{4M_P^2}\left[\phi_f^2 - \phi_e^2 + \frac{C}{4\phi_c^2}\left(\phi_f^4 - \phi_e^4\right)\right], \tag{3.5}$$

by which one can readily find

$$4M_P^2 \delta\mathcal{N}_f(n_f) = \delta(\phi_f^2)\left(1 + \frac{C}{2}\frac{\phi_f^2}{\phi_c^2}\right) . \tag{3.6}$$

On the other hand using Eq. (2.9) one has

$$-\,4M_P^2 \delta n_f \simeq \delta\left(\phi_f^2\right)\left(1 + \frac{C}{2}\frac{\phi_c^2}{\phi_f^2}\right) . \tag{3.7}$$

By using the fact that $\phi_f^2 \simeq \phi_c^2 - 4M_P^2 n_f$ one can find that

$$\delta\mathcal{N}_f(n_f) \simeq -\,\delta n_f \left(1 - 2C\epsilon n_f\right) \quad \to \quad \frac{d\mathcal{N}_f}{dn_f} = -1 + 2C\epsilon\, n_f, \tag{3.8}$$

in which ϵ denotes the conventional slow-roll parameter which is approximately given by $\epsilon \simeq 2M_P^2/\phi_c^2$.

Now we trace back the evolution to earlier times before the end of transition, $\mathcal{N} > \mathcal{N}_f$. For this stage, instead of $\mathcal{N}$, it is more convenient to use n which is the number of e-folds from the critical point counted *forward* in time, i.e., $n = n_f + \mathcal{N}_f - \mathcal{N}$. Then $\chi^2(n)$ is given by

$$\chi^2(n) = \exp\left[2\left(f(n) - f(n_f)\right)\right]\chi^2_{min}(n_f)\,, \tag{3.9}$$

where $f(n)$ for a sharp phase transition is given by

$$f(n) = \frac{2}{3}\epsilon_\chi\, n^{3/2}\,. \tag{3.10}$$

During this era, n is expressed in terms of $\phi(n)$ as given by Eq. (2.9),

$$-\,4M_P^2\, n = \phi(n)^2 - \phi_c^2\left[1 - C\ln\left(\frac{\phi}{\phi_c}\right)\right] . \tag{3.11}$$

Here we note that n depends on n_f and $\mathcal{N}$ in a non-trivial way,

$$n(n_f, \mathcal{N}) = n_f + \mathcal{N}_f(n_f) - \mathcal{N}\,. \tag{3.12}$$

By virtue of the above geometric relation and by using Eq. (3.8) one has

$$\frac{\partial n}{\partial n_f} = 2C\epsilon\, n_f\,. \tag{3.13}$$

Keeping in mind the above dependence of n on n_f and $\mathcal{N}$, let us take the variation of Eqs. (3.9) and (3.11). We obtain

$$\begin{aligned} \frac{\delta\chi^2(n)}{\langle\delta\chi^2(n)\rangle} &= \frac{\delta\chi^2_{min}(n_f)}{\chi^2_{min}(n_f)} + 2f'(n)\delta\, n - 2f'(n_f)\delta\, n_f\,, && (3.14)\\ -2M_p^2\delta n &\simeq \phi(n)\delta\phi(n)\left(1+\frac{C}{2}+C\,\epsilon\, n\right)\,. && (3.15) \end{aligned}$$

On the other hand from Eq. (3.4), one finds

$$\chi^2_{min}(n_f) = 4M_P^2\frac{g^2}{\lambda}\, n_f\,, \tag{3.16}$$

where we have used Eq. (2.9) and the fact that $\phi_f \lesssim \phi_c$. This results in

$$\frac{\delta\chi^2_{min}(n_f)}{\chi^2_{min}(n_f)} = \frac{\delta n_f}{n_f}\,. \tag{3.17}$$

Finally, solving Eqs. (3.14) and (3.15) for $\delta\mathcal{N}$, we find

$$\delta\mathcal{N} = \frac{\delta\chi^2(n)}{\langle\delta\chi^2(n)\rangle}\frac{\partial n}{\partial n_f}\frac{1}{-2f'(n_f)+n_f^{-1}} + \frac{\phi\,\delta\phi(n)}{2M_P^2}\left[1+\frac{C}{2}+C\epsilon n + \frac{2f'(n)}{-2f'(n_f)+n_f^{-1}}\frac{\partial n}{\partial n_f}\right]\,. \tag{3.18}$$

To simplify the above relation we note that $2n_f f'(n_f) \gg 1$ which is valid in our model with a sharp phase transition. Then the above expression reduces to

$$\delta\mathcal{N} = -\frac{C\epsilon\, n_f}{f'(n_f)}\frac{\delta\chi^2(n)}{\langle\delta\chi^2(n)\rangle} + \left[1+\frac{C}{2}+C\epsilon(n-2n_f)\right]\frac{\phi\delta\phi}{2M_P^2}\,. \tag{3.19}$$

Noting that $\delta\chi^2(n)$ and $\langle\chi^2(n)\rangle$ have the same n-dependence the final result for the comoving curvature perturbation $\mathcal{R}_c = \delta\mathcal{N}$ can be expressed in terms of $\delta\chi^2(0)$ and $\langle\chi^2(0)\rangle$,

$$\mathcal{R} = \delta\mathcal{N} = -\frac{C\epsilon\, n_f}{f'(n_f)}\frac{\delta\chi^2(0)}{\langle\delta\chi^2(0)\rangle} + \left[1+\frac{C}{2}+C\epsilon(n-2n_f)\right]\frac{\phi\delta\phi}{2M_P^2}\,, \tag{3.20}$$

where and below we omit the suffix c from $\mathcal{R}_c$ and simply denote it by $\mathcal{R}$ for notational simplicity.

This is our key formula for computing the power spectrum and bispectrum. As can be seen from the above expression, the curvature perturbation has the conventional inflaton contribution up to slow-roll corrections in the inflaton mass and the contribution from the waterfall field. The latter is a dynamical effect which is intrinsic to our model, in contrast to many other models in which local features are added simply phenomenologically.

IV. POWER SPECTRUM OF CURVATURE PERTURBATIONS

Having found the final curvature perturbations with the δN formalism we now calculate the power spectrum. Our aim is to find an imprint of the sharp waterfall transition on the power spectrum.

As clear from Eq. (3.20), the power spectrum can be divided into two distinct contributions, the one from the inflaton and the other from the waterfall field,

$$\begin{aligned} \mathcal{P}_\mathcal{R} &= \mathcal{P}_\mathcal{R}^{wf} + \mathcal{P}_\mathcal{R}^{\phi}\\ &= \frac{C^2\epsilon^2 n_f^2}{f'^2(n_f)}\,\mathcal{P}_{\delta\chi^2/\chi^2} + \left[1+\frac{C}{2}+\mathcal{O}(C\epsilon)\right]^2\frac{\phi^4}{4M_P^4}\,\mathcal{P}_{\delta\phi/\phi}\,. && (4.1) \end{aligned}$$

Below we evaluate each contribution separately.

A. Contribution of the inflaton to the power spectrum

Since the inflaton field is light throughout the whole stage of inflation the amplitude of its quantum fluctuations on flat hypersurface at the time of horizon crossing is given by the usual formula,

$$\delta\phi(k) = \frac{H(n_k)}{\sqrt{2k^3}}\,, \tag{4.2}$$

where $H(n_k)$ is the Hubble parameter at the time of horizon crossing. This gives

$$\mathcal{P}_{\mathcal{R}}^{\phi}(k) \simeq \frac{1}{4\pi^2}\left[1+\frac{C}{2}\right]^2 \frac{\phi^2 H^2}{4M_P^4}\bigg|_{n=n_k} \simeq \frac{(1+C)}{48\pi^2}\,\frac{\phi^2\, V_{eff}^{+}(\phi)}{M_P^6}\bigg|_{n=n_k}\,, \tag{4.3}$$

where $V_{eff}^{+}(\phi)$ is given by Eq. (2.8), which may be rewritten to first order in C as

$$V_{eff}^{+}(\phi) = \frac{1}{2}m^2\,(1+C)\left(1-\frac{C}{2}\frac{\phi^2}{\phi_c^2}\right)\phi^2 + O(C\,\epsilon)\,. \tag{4.4}$$

Thus we obtain

$$\mathcal{P}_{\mathcal{R}}^{\phi}(k) = \frac{1}{96\pi^2}\,(1+C)^2\left(1-\frac{C}{2}\frac{\phi^2}{\phi_c^2}\right)\frac{m^2\phi^4}{M_P^6}\bigg|_{n=n_k}\,. \tag{4.5}$$

Neglecting the corrections of $O(C)$, the above expression reduces to the standard formula, $\mathcal{P}_{\mathcal{R}}^{\phi}(k) = V^3/(12\pi^2 V'^2 M_P^6)|_{n=n_k}$.

B. Contribution of the waterfall to the power spectrum

Now we calculate the contribution of the waterfall field perturbations to the power spectrum. In order to estimate this contribution we first note that

$$\Big\langle \left(\delta\chi^2\right)_{\mathbf{k}}\left(\delta\chi^2\right)_{\mathbf{q}}\Big\rangle \;\equiv\; P_{\delta\chi^2}(k)(2\pi)^3\delta^3(\mathbf{k}+\mathbf{q}). \tag{4.6}$$

$$\mathcal{P}_{\delta\chi^2/\chi^2}(k) \;\equiv\; \frac{1}{\langle\delta\chi^2(0)\rangle^2}\,\frac{k^3}{2\pi^2}P_{\delta\chi^2}(k)\,. \tag{4.7}$$

The correlation function of $\delta\chi^2_{\mathbf{k}}$ can be calculated using the identity [32],

$$\Big\langle \left(\delta\chi^2\right)_{k}\left(\delta\chi^2\right)_{q}\Big\rangle \;=\; 2\int\frac{d^3q}{(2\pi)^3}|\delta\chi_{|\mathbf{k}-\mathbf{q}|}|^2|\delta\chi_q|^2\;(2\pi)^3\delta^3(\mathbf{k}+\mathbf{q})\,. \tag{4.8}$$

In Appendix B we show that

$$\mathcal{P}_{\delta\chi^2}(k) \simeq \frac{\xi^3 H^2}{4\pi^2}\,\mathcal{P}_{\delta\chi}\,, \tag{4.9}$$

where ξ is a numerical factor of order unity. This means that the power spectrum of $\delta\chi^2$ is proportional to the power spectrum of $\delta\chi$. Plugging this into Eqs. (4.1) and (4.7) and using the explicit form of $f(n)$ given in Eq. (3.10) and $\langle\delta\chi^2(0)\rangle$ calculated in Eq. (A11), we find

$$\mathcal{P}_{\mathcal{R}}^{wf}(k) = \frac{4C^2\epsilon^2 n_f\xi^3}{3\epsilon_\chi^{10/3}}\,\frac{\mathcal{P}_{\delta\chi}(k;0)}{\langle\delta\chi^2(0)\rangle}\,. \tag{4.10}$$

Finally, plugging the waterfall field perturbation spectrum (2.33) to the above, we obtain

$$\mathcal{P}_{\mathcal{R}}^{wf}(k) \simeq \begin{cases} \dfrac{16}{9}C^2\epsilon^2 n_f\,\epsilon_\chi^{-20/3}\,\xi^3\left(\dfrac{k}{k_c}\right)^3\,; & k<k_c\,,\\[2ex] \dfrac{16}{9}C^2\epsilon^2 n_f\,\epsilon_\chi^{-8/3}\,\xi^3 n_t(k)\exp\left[-\tfrac{4}{3}\epsilon_\chi n_t^{3/2}(k)\right]\,; & k>k_c\,. \end{cases} \tag{4.11}$$

C. Total curvature perturbation spectrum

We now consider the total curvature perturbation spectrum by adding contributions both from the inflaton field and the waterfall field. Since the waterfall contribution is peaked at $k = k_{max} \gtrsim k_c$, let us first compare the amplitudes of $\mathcal{P}_{\mathcal{R}}^{wf}(k)$ and $\mathcal{P}_{\mathcal{R}}^{\phi}(k)$ at $k \simeq k_{max}$. Using Eq. (2.35) for k_{max} and comparing Eqs. (4.11) and (4.5), we find

$$\frac{\mathcal{P}_{\mathcal{R}}^{wf}(k_{max})}{\mathcal{P}_{\mathcal{R}}^{\phi}} \simeq 10^3 C^2 \left(\frac{\epsilon}{10^{-2}}\right)^4 \left(\frac{\epsilon_\chi}{10}\right)^{-10/3}, \tag{4.12}$$

where the approximation $m/M_P \sim 10^{-6}$ has been used in order to satisfy the COBE normalization. This result shows that there can be a prominent peak even for a small C, say $C \sim 0.1$.

In Fig. 2 we plot the total curvature perturbation power spectrum for the parameters $C = 0.15$, $\epsilon = 0.01$ and $\epsilon_\chi = 20$. The peak at $k = k_{max} \sim k_c$ in the spectrum is due to the waterfall field contribution, $\mathcal{P}_{\mathcal{R}}^{wf}(k)$. The spectrum away from the peak is dominated by the inflaton contribution, $\mathcal{P}_{\mathcal{R}}^{\phi}(k)$.

In passing, it is instructive to estimate n_f, the duration of the phase transition. As mentioned before, we treat $\langle\delta\chi^2\rangle$ as the averaged classical value of the waterfall field on each horizon size patch. A good criterion for the completion of the phase transition is when $\langle\delta\chi^2\rangle$ reaches the value of its local minimum $\chi^2_{min}(n_f)$ given by Eq. (3.4). With the help of Eq. (3.11), we find

$$\langle\delta\chi^2(n_f)\rangle \simeq \frac{4g^2M_P^2}{\lambda}\, n_f\,. \tag{4.13}$$

In Appendix A the expectation value $\langle\delta\chi^2(n)\rangle$ is evaluated as

$$\langle\delta\chi^2(n)\rangle = \langle\delta\chi^2(0)\rangle \exp(\frac{4}{3}\epsilon_\chi n^{3/2}) \simeq \frac{3\epsilon_\chi^{4/3}H^2}{16\pi^2}\exp(\frac{4}{3}\epsilon_\chi n^{3/2})\,. \tag{4.14}$$

Equating this with $\chi^2_{min}(n_f)$, we obtain an estimate,

$$n_f = \Gamma\,\epsilon_\chi^{-2/3}\,; \quad \Gamma \simeq \left(\ln\left[\frac{32\pi^2\epsilon_\chi^{2/3}}{6\lambda}\right]\right)^{2/3}. \tag{4.15}$$

For our numerical example we find $n_f \simeq 0.5$ so the phase transition is fairly sharp. But it is smooth enough to render the dynamics of the phase transition adiabatic. Namely, we are free from possible violations of the adiabaticity of the inflaton vacuum state that may occur for very sharp transitions as discussed in the literature [2–6, 9, 10, 14, 18, 19].

V. BISPECTRUM AND NON-GAUSSIANITIES

Now we compute the bispectrum of this model. Due to the intrinsic non-Gaussian nature of $\delta\chi^2$, we expect to see large spiky non-Gaussianities when $\mathcal{P}_{\mathcal{R}}^{wf}(k_{max}) > \mathcal{P}_{\mathcal{R}}^{\phi}(k_{max})$.

So far in our analysis, we have expanded δN up to $\delta\chi^2$ as given by Eq. (3.20). In order to calculate the bispectrum we need to expand δN up to $\delta\chi^4$. This is done in Appendix C. The three point function can be read from Eq. (C3) as

$$\begin{aligned}\langle\mathcal{R}_{\mathbf{k}_1}\mathcal{R}_{\mathbf{k}_2}\mathcal{R}_{\mathbf{k}_3}\rangle &\equiv B_{\mathcal{R}}(\mathbf{k}_1,\mathbf{k}_2,\mathbf{k}_3)(2\pi)^3\delta(\mathbf{k}_1+\mathbf{k}_2+\mathbf{k}_3)\\ &= (N_{,\chi^2})^3\Big\langle\left(\delta\chi^2\right)_{\mathbf{k}_1}\left(\delta\chi^2\right)_{\mathbf{k}_2}\left(\delta\chi^2\right)_{\mathbf{k}_3}\Big\rangle\\ &+ \frac{1}{2}(N_{,\chi^2})^2N_{,\chi^2,\chi^2}\Big\langle\left[\left(\Delta\chi^2\right)^2\right]_{\mathbf{k}_1}\left(\delta\chi^2\right)_{\mathbf{k}_2}\left(\delta\chi^2\right)_{\mathbf{k}_3} + \text{c.p.}\Big\rangle\\ &+ \frac{1}{2}(N_{,\phi})^2N_{,\phi\,\phi}\Big\langle\left(\delta\phi^2\right)_{\mathbf{k}_1}\delta\phi_{\mathbf{k}_2}\delta\phi_{\mathbf{k}_3} + \text{c.p.}\Big\rangle\,,\end{aligned} \tag{5.1}$$

where c.p. represents cyclic permutations, $(\mathbf{k}_1,\mathbf{k}_2,\mathbf{k}_3) \to (\mathbf{k}_2,\mathbf{k}_3,\mathbf{k}_1) \to (\mathbf{k}_3,\mathbf{k}_1,\mathbf{k}_2)$ and $\Delta\chi^2$ is the fluctuations of $\delta\chi^2(n,\mathbf{x})$ on scales larger than the horizon scale, as defined in Eq. (2.14).

There are two distinct contributions to the three point function. The first term in Eq. (5.1) is due to the intrinsic non-Gaussianity of $\delta\chi^2$. We define the intrinsic bispectrum of $\delta\chi^2$ in the standard way by

$$\Big\langle(\delta\chi^2)_{\mathbf{k}_1}(\delta\chi^2)_{\mathbf{k}_2}(\delta\chi^2)_{\mathbf{k}_3}\Big\rangle = B_{\delta\chi^2}(k_1,k_2,k_3)(2\pi)^3\delta^3(\mathbf{k}_1+\mathbf{k}_2+\mathbf{k}_3)\,. \tag{5.2}$$

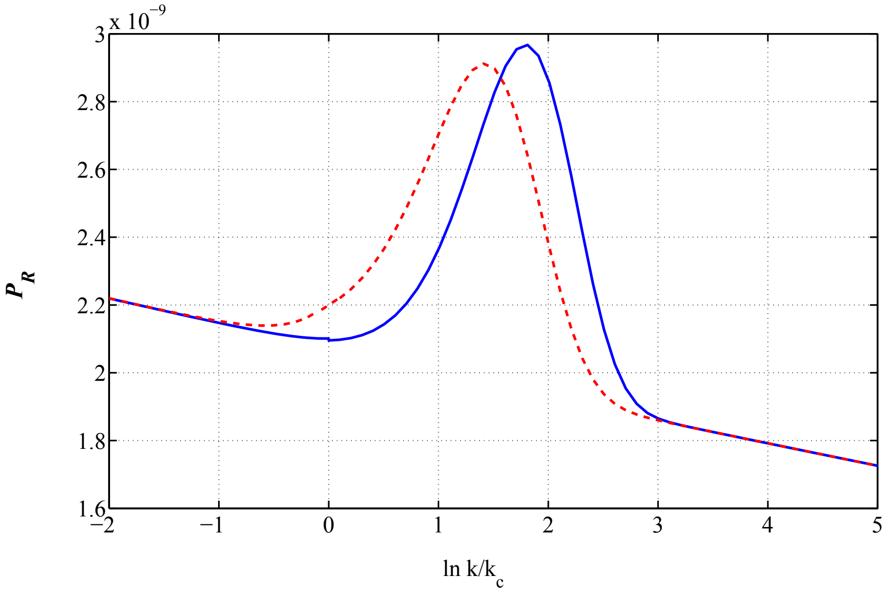

FIG. 2: Power spectrum of the curvature perturbation. The dashed red curve shows an analytical estimate of the total curvature perturbation power spectrum by adding both the inflaton and waterfall field contributions, $\mathcal{P}_{\mathcal{R}}^{\phi}(k)+\mathcal{P}_{\mathcal{R}}^{wf}(k)$, given by Eqs. (4.5) and (4.11). The blue solid curve shows the total curvature perturbation, $\mathcal{P}_{\mathcal{R}}(k)$, in which the convolution integral Eq. (4.8) is numerically calculated. As one can see in this figure, $\mathcal{P}_{\mathcal{R}}^{wf}(k)$ peaks near $k_{max}\sim k_c$ and decays quickly for k not close to k_{max}. The parameters are the same as in Fig. 1.

The second term in Eq. (5.1) is due to nonlinear dynamics of the waterfall field, while the last term is that of the inflaton field which generically gives a negligible contribution when the inflaton is slow-rolling. Below we compute the first and second terms separately.

A. Dynamically generated bispectrum

Let us first concentrate on the second term,

$$\langle \mathcal{R}_{\mathbf{k}_1}\mathcal{R}_{\mathbf{k}_2}\mathcal{R}_{\mathbf{k}_3}\rangle_{(2)} \equiv \frac{1}{2}(N_{,\chi^2})^2 N_{,\chi^2,\chi^2}\left\langle \left[\left(\Delta\chi^2\right)^2\right]_{\mathbf{k}_1}\left(\delta\chi^2\right)_{\mathbf{k}_2}\left(\delta\chi^2\right)_{\mathbf{k}_3}+\text{c.p.}\right\rangle . \tag{5.3}$$

Here we have intentionally avoided to call the above the dynamically generated bispectrum, because we shall see that it also includes some contribution from the intrinsic bispectrum of $\delta\chi^2$.

By noting that

$$\left[\left(\Delta\chi^2\right)^2\right]_{\mathbf{k}} = \left(\delta\chi^4\right)_{\mathbf{k}} - 2\langle\delta\chi^2\rangle\left(\delta\chi^2\right)_{\mathbf{k}}\,, \tag{5.4}$$

one has

$$\begin{aligned}
&\left\langle \left[\left(\Delta\chi^2\right)^2\right]_{\mathbf{k}_1}\left(\delta\chi^2\right)_{\mathbf{k}_2}\left(\delta\chi^2\right)_{\mathbf{k}_3}+\text{c.p.}\right\rangle \\
&\quad= -2\times 3\times\langle\delta\chi^2\rangle\left\langle \left(\delta\chi^2\right)_{\mathbf{k}_1}\left(\delta\chi^2\right)_{\mathbf{k}_2}\left(\delta\chi^2\right)_{\mathbf{k}_3}\right\rangle + \left[\left\langle \left(\delta\chi^4\right)_{\mathbf{k}_1}\left(\delta\chi^2\right)_{\mathbf{k}_2}\left(\delta\chi^2\right)_{\mathbf{k}_3}\right\rangle+\text{c.p.}\right] \\
&\quad= -6\langle\delta\chi^2\rangle B_{\delta\chi^2}(k_1,k_2,k_3)\,(2\pi)^3\delta^3(\mathbf{k}_1+\mathbf{k}_2+\mathbf{k}_3) + \left[\left\langle(\delta\chi^4)_{\mathbf{k}_1}(\delta\chi^2)_{\mathbf{k}_2}(\delta\chi^2)_{\mathbf{k}_3}\right\rangle+\text{c.p.}\right].
\end{aligned} \tag{5.5}$$

The first term on the right hand side above, proportional to $B_{\delta\chi^2}$, is of the same form as the first term in Eq. (5.1), which we evaluate later. Here we first focus on the other terms in the square brackets.

We note that if $\delta\chi^2$ were Gaussian, we could express these terms in terms of the product of two point correlation functions. But since this is not the case for $\delta\chi^2$, there is also a contribution proportional to the three point correlation function of $\delta\chi^2$, as we shall see below.

By expanding $\delta\chi^4$ one has

$$\left\langle \left(\delta\chi^4\right)_{\mathbf{k}_1} \left(\delta\chi^2\right)_{\mathbf{k}_2} \left(\delta\chi^2\right)_{\mathbf{k}_3} \right\rangle = \int \widetilde{d^3q} \left\langle \left(\delta\chi^2\right)_{\mathbf{k}_1-\mathbf{q}} \left(\delta\chi^2\right)_{\mathbf{q}} \left(\delta\chi^2\right)_{\mathbf{k}_2} \left(\delta\chi^2\right)_{\mathbf{k}_3} \right\rangle , \tag{5.6}$$

in which we have introduced $\widetilde{d^3q} = d^3q/(2\pi)^3$ to simplify the notation. To calculate the r.h.s of this equation we should first classify possible contractions. Since we are not interested in tad-pole type graphs but only in irreducible graphs, there are some restrictions on non-trivial contractions. First, contractions between the terms within any of $(\delta\chi^2)_{\mathbf{p}}$ themselves are not allowed. Second, contractions should not be closed only within the terms in $(\delta\chi^4)_{\mathbf{k}_1}$, corresponding to the first two terms in the r.h.s. of the equation. Then one finds there are two different classes of contractions. The first class is in which there is one contraction between a pair of terms in $(\delta\chi^4)_{\mathbf{k}_1}$. The second class is in which there is no contraction between any pair of terms in $(\delta\chi^4)_{\mathbf{k}_1}$ themselves.

Let us consider the first class and count the number of possible contractions. There are 4 choices to choose a pair in $(\delta\chi^4)_{\mathbf{k}_1}$. Then one of the remaining two $\delta\chi$ has 4 choices to contract with one of $\delta\chi$ in $(\delta\chi^2)_{\mathbf{k}_2}$ and $(\delta\chi^2)_{\mathbf{k}_3}$, and the last $\delta\chi$ in $(\delta\chi^4)_{\mathbf{k}_1}$ has 2 choices to contract the remaining terms in $(\delta\chi^2)_{\mathbf{k}_2}$ and $(\delta\chi^2)_{\mathbf{k}_3}$. Thus there are in total $4 \times 4 \times 2 = 32$ possible contractions in the first class. They all give the same result. So let us calculate one of them:

$$\begin{aligned}
&\int \widetilde{d^3q} \prod_i \widetilde{d^3p_i} \left\langle \Big(\delta\chi_{\mathbf{k}_1-\mathbf{p}_1-\mathbf{q}} \delta\chi_{\mathbf{p}_1} \big) \big(\delta\chi_{\mathbf{q}-\mathbf{p}_2} \delta\chi_{\mathbf{p}_2} \big) \big(\delta\chi_{\mathbf{k}_2-\mathbf{p}_3} \delta\chi_{\mathbf{p}_3} \big) \big(\delta\chi_{\mathbf{k}_3-\mathbf{p}_4} \delta\chi_{\mathbf{p}_4} \Big) \right\rangle \\
&= \int \widetilde{d^3q} \prod_i d^3p_i \, |\delta\chi_{|\mathbf{q}-\mathbf{p}_2|}|^2 |\delta\chi_{p_1}|^2 |\delta\chi_{p_2}|^2 |\delta\chi_{p_3}|^2 \times \delta\text{-factor} \, ,
\end{aligned} \tag{5.7}$$

where

$$\delta\text{-factor} = \delta^3(\mathbf{k}_1 - \mathbf{p}_1 - \mathbf{p}_2)\delta^3(\mathbf{k}_2 + \mathbf{p}_1 - \mathbf{p}_3)\delta^3(\mathbf{k}_3 + \mathbf{p}_2 - \mathbf{p}_4)\delta^3(\mathbf{p}_3 + \mathbf{p}_4) \, . \tag{5.8}$$

Performing first the integrals over $\mathbf{p}_2$, $\mathbf{p}_3$ and $\mathbf{p}_4$, and then over $\mathbf{q}$, the above reduces to

$$\begin{aligned}
&\int \widetilde{d^3q} \int d^3p_1 \, |\delta\chi_{|\mathbf{q}+\mathbf{p}_1-\mathbf{k}_1|}|^2 |\delta\chi_{p_1}|^2 |\delta\chi_{|\mathbf{k}_2+\mathbf{p}_1|}|^2 |\delta\chi_{|\mathbf{k}_1-\mathbf{p}_1|}|^2 \delta^3(\mathbf{k}_1 + \mathbf{k}_2 + \mathbf{k}_3) \\
&= \langle \delta\chi^2 \rangle \int d^3p_1 \, |\delta\chi_{p_1}|^2 |\delta\chi_{|\mathbf{k}_2+\mathbf{p}_1|}|^2 |\delta\chi_{|\mathbf{k}_1-\mathbf{p}_1|}|^2 \, \delta^3(\mathbf{k}_1 + \mathbf{k}_2 + \mathbf{k}_3) \\
&= \frac{1}{8} \langle \delta\chi^2 \rangle \big\langle \left(\delta\chi^2\right)_{\mathbf{k}_1} \left(\delta\chi^2\right)_{\mathbf{k}_2} \left(\delta\chi^2\right)_{\mathbf{k}_3} \big\rangle \, ,
\end{aligned} \tag{5.9}$$

where we have used the fact that [32]

$$\big\langle \left(\delta\chi^2\right)_{\mathbf{k}_1} \left(\delta\chi^2\right)_{\mathbf{k}_2} \left(\delta\chi^2\right)_{\mathbf{k}_3} \big\rangle = 8 \int d^3p_1 \, |\delta\chi_{p_1}|^2 |\delta\chi_{|\mathbf{k}_2+\mathbf{p}_1|}|^2 |\delta\chi_{|\mathbf{k}_1-\mathbf{p}_1|}|^2 \delta^3(\mathbf{k}_1 + \mathbf{k}_2 + \mathbf{k}_3) \, . \tag{5.10}$$

Thus we obtain

$$\begin{aligned}
&\int \widetilde{d^3q} \prod_i \widetilde{d^3p_i} \langle \big(\delta\chi_{\mathbf{k}_1-\mathbf{p}_1-\mathbf{q}} \delta\chi_{\mathbf{p}_1} \big) \big(\delta\chi_{\mathbf{q}-\mathbf{p}_2} \delta\chi_{\mathbf{p}_2} \big) \big(\delta\chi_{\mathbf{k}_2-\mathbf{p}_3} \delta\chi_{\mathbf{p}_3} \big) \big(\delta\chi_{\mathbf{k}_3-\mathbf{p}_4} \delta\chi_{\mathbf{p}_4} \big) \rangle \\
&= \frac{1}{8} \langle \delta\chi^2 \rangle B_{\delta\chi^2}(k_1, k_2, k_3) \, (2\pi)^3 \delta^3(\mathbf{k}_1 + \mathbf{k}_2 + \mathbf{k}_3) \, ,
\end{aligned} \tag{5.11}$$

where the bispectrum $B_{\delta\chi^2}(k_1, k_2, k_3)$ is defined in Eq. (5.2). Since there are 32×3 of the same terms, the contribution from this class amounts to

$$\begin{aligned}
\Big[\langle (\delta\chi^4)_{\mathbf{k}_1} (\delta\chi^2)_{\mathbf{k}_2} (\delta\chi^2)_{\mathbf{k}_3} \rangle + \text{c.p.} \Big]_{\text{1st}} &= 32 \times 3 \times \frac{1}{8} \langle \delta\chi^2 \rangle B_{\delta\chi^2}(k_1, k_2, k_3) \, (2\pi)^3 \delta^3(\mathbf{k}_1 + \mathbf{k}_2 + \mathbf{k}_3) \\
&= 12 \, \langle \delta\chi^2 \rangle B_{\delta\chi^2}(k_1, k_2, k_3) \, (2\pi)^3 \delta^3(\mathbf{k}_1 + \mathbf{k}_2 + \mathbf{k}_3) \, .
\end{aligned} \tag{5.12}$$

Let us now turn to the second class, in which every $\delta\chi$ in $(\delta\chi^4)_{\mathbf{k}_1}$ is contracted with one of $\delta\chi$ in either $(\delta\chi^2)_{\mathbf{k}_2}$ or $(\delta\chi^2)_{\mathbf{k}_3}$. Hence, there are $4\times 3\times 2 = 24$ possible contractions. Again they all give the same result. One of them is given by

$$
\begin{aligned}
&\int \widetilde{d^3q}\prod_i \widetilde{d^3p_i}\left\langle \left(\delta\chi_{\mathbf{k}_1-\mathbf{p}_1-\mathbf{q}}\delta\chi_{\mathbf{p}_1}\right)\left(\delta\chi_{\mathbf{q}-\mathbf{p}_2}\delta\chi_{\mathbf{p}_2}\right)\left(\delta\chi_{\mathbf{k}_2-\mathbf{p}_3}\delta\chi_{\mathbf{p}_3}\right)\left(\delta\chi_{\mathbf{k}_3-\mathbf{p}_4}\delta\chi_{\mathbf{p}_4}\right)\right\rangle \\
&= \int \widetilde{d^3q}\prod_i d^3p_i\,|\delta\chi_{|\mathbf{k}_2-\mathbf{p}_3|}|^2|\delta\chi_{p_1}|^2|\delta\chi_{p_2}|^2|\delta\chi_{p_3}|^2\times\delta\text{-factor}\,, \qquad (5.13)
\end{aligned}
$$

where

$$
\delta\text{-factor} = \delta^3(\mathbf{k}_1+\mathbf{k}_2-\mathbf{p}_1-\mathbf{p}_3-\mathbf{q})\delta^3(\mathbf{k}_3+\mathbf{p}_1-\mathbf{p}_4)\delta^3(\mathbf{q}-\mathbf{p}_2+\mathbf{p}_3)\delta^3(\mathbf{p}_2+\mathbf{p}_4)\,. \qquad (5.14)
$$

Performing first the integrals over $\mathbf{p}_2$, $\mathbf{p}_3$ and $\mathbf{p}_4$, and then over $\mathbf{q}$ gives

$$
\begin{aligned}
&\int \widetilde{d^3p_1}\,|\delta\chi_{p_1}|^2|\delta\chi_{|\mathbf{k}_3+\mathbf{p}_1|}|^2\int d^3q|\delta\chi_{|\mathbf{q}+\mathbf{p}_1-\mathbf{k}_1|}|^2|\delta\chi_{|\mathbf{q}+\mathbf{p}_1+\mathbf{k}_3|}|^2\,\delta^3(\mathbf{k}_1+\mathbf{k}_2+\mathbf{k}_3) \\
&= \frac{1}{4}P_{\delta\chi^2}(k_2)\,P_{\delta\chi^2}(k_3)\,(2\pi)^3\delta^3(\mathbf{k}_1+\mathbf{k}_2+\mathbf{k}_3)\,, \qquad (5.15)
\end{aligned}
$$

where we have used the definition of $P_{\delta\chi^2}$, Eq. (4.6). Since there are 24 of them, plus cyclic permutations, the contribution from this class is in total,

$$
\begin{aligned}
&\left[\left\langle(\delta\chi^4)_{\mathbf{k}_1}(\delta\chi^2)_{\mathbf{k}_2}(\delta\chi^2)_{\mathbf{k}_3}\right\rangle + \text{c.p.}\right]_{\text{2nd}} \\
&= 24\times\frac{1}{4}\Big[P_{\delta\chi^2}(k_2)\,P_{\delta\chi^2}(k_3)+\text{c.p.}\Big]\,(2\pi)^3\delta^3(\mathbf{k}_1+\mathbf{k}_2+\mathbf{k}_3) \\
&= 6\Big[P_{\delta\chi^2}(k_1)\,P_{\delta\chi^2}(k_2)+\text{c.p.}\Big]\,(2\pi)^3\delta^3(\mathbf{k}_1+\mathbf{k}_2+\mathbf{k}_3)\,. \qquad (5.16)
\end{aligned}
$$

Adding up all the contributions given by Eqs. (5.12) and (5.16) together with the first term in (5.5), we obtain

$$
\begin{aligned}
&\Big\langle\left[(\Delta\chi^2)^2\right]_{\mathbf{k}_1}(\delta\chi^2)_{\mathbf{k}_2}(\delta\chi^2)_{\mathbf{k}_3}+\text{c.p.}\Big\rangle \\
&= 6\left(\langle\delta\chi^2\rangle B_{\delta\chi^2}(k_1,k_2,k_3)+\Big[P_{\delta\chi^2}(k_1)\,P_{\delta\chi^2}(k_2)+\text{c.p.}\Big]\right)\,(2\pi)^3\delta^3(\mathbf{k}_1+\mathbf{k}_2+\mathbf{k}_3)\,. \qquad (5.17)
\end{aligned}
$$

Substituting the above in Eq. (5.3), the three point correlation function of the curvature perturbation can be represented in terms of the power spectrum and bispectrum of $\delta\chi^2$ as

$$
\begin{aligned}
\langle\mathcal{R}_{\mathbf{k}_1}\mathcal{R}_{\mathbf{k}_2}\mathcal{R}_{\mathbf{k}_3}\rangle_{(2)} = \Bigg[&3(N_{,\chi^2})^2N_{,\chi^2\chi^2}\langle\delta\chi^2\rangle B_{\delta\chi^2}(k_1,k_2,k_3) \\
&+3(N_{,\chi^2})^2N_{,\chi^2\chi^2}\Big(P_{\delta\chi^2}(k_1)\,P_{\delta\chi^2}(k_2)+\text{c.p.}\Big)\Bigg]\,(2\pi)^3\delta^3\left(\mathbf{k}_1+\mathbf{k}_2+\mathbf{k}_3\right)\,. \qquad (5.18)
\end{aligned}
$$

As it is clear in the above result, while the second term is an ordinary nonlinear interaction term with the vertex proportional to $N_{,\chi^2\chi^2}$, which can be easily evaluated, the first term is due to the intrinsic non-Gaussianity of the $\delta\chi^2$ field which needs to be computed.

The above equation can be further simplified by using Eq. (C4) and noting that $P_{\mathcal{R}}^{wf} = N_{,\chi^2}^2P_{\delta\chi^2}$,

$$
\langle\mathcal{R}_{\mathbf{k}_1}\mathcal{R}_{\mathbf{k}_2}\mathcal{R}_{\mathbf{k}_3}\rangle_{(2)} = -3(N_{,\chi^2})^3B_{\delta\chi^2}(k_1,k_2,k_3)(2\pi)^3\delta^3\left(\mathbf{k}_1+\mathbf{k}_2+\mathbf{k}_3\right)+\langle\mathcal{R}_{\mathbf{k}_1}\mathcal{R}_{\mathbf{k}_2}\mathcal{R}_{\mathbf{k}_3}\rangle_{dyn}\,, \qquad (5.19)
$$

where we have defined the dynamically generated bispectrum of the curvature perturbation by

$$
\begin{aligned}
\langle\mathcal{R}_{\mathbf{k}_1}\mathcal{R}_{\mathbf{k}_2}\mathcal{R}_{\mathbf{k}_3}\rangle_{dyn} &= B_{\mathcal{R}}^{dyn}(\mathbf{k}_1,\mathbf{k}_2,\mathbf{k}_3)(2\pi)^3\delta^3\left(\mathbf{k}_1+\mathbf{k}_2+\mathbf{k}_3\right) \\
&\equiv 3\frac{N_{,\chi^2\chi^2}}{(N_{,\chi^2})^2}\Big(P_{\mathcal{R}}^{wf}(k_1)P_{\mathcal{R}}^{wf}(k_2)+\text{c.p.}\Big)(2\pi)^3\delta^3\left(\mathbf{k}_1+\mathbf{k}_2+\mathbf{k}_3\right)\,. \qquad (5.20)
\end{aligned}
$$

B. Bispectrum from intrinsic non-Gaussianity

Now we evaluate the bispectrum from the intrinsic non-Gaussianity of $\delta\chi^2$. From Eqs. (5.1) and (5.19), we have

$$\begin{aligned}\langle \mathcal{R}_{\mathbf{k}_1}\mathcal{R}_{\mathbf{k}_2}\mathcal{R}_{\mathbf{k}_3}\rangle_{int} &= B^{int}_{\mathcal{R}}(\mathbf{k}_1,\mathbf{k}_2,\mathbf{k}_3)(2\pi)^3\delta(\mathbf{k}_1+\mathbf{k}_2+\mathbf{k}_3) \\ &\equiv -2(N_{,\chi^2})^3 B_{\delta\chi^2}(\mathbf{k}_1,\mathbf{k}_2,\mathbf{k}_3)(2\pi)^3\delta^3\left(\mathbf{k}_1+\mathbf{k}_2+\mathbf{k}_3\right)\,. \end{aligned} \tag{5.21}$$

Following [32], we obtain an expression for the bispectrum of $\delta\chi^2$ as

$$B_{\delta\chi^2}(k_1,k_2,k_3) = 8\int \widetilde{d^3q}\,|\delta\chi_q|^2|\delta\chi_{|\mathbf{k}_1-\mathbf{q}|}|^2|\delta\chi_{|\mathbf{k}_2+\mathbf{q}|}|^2\,. \tag{5.22}$$

It is hard to calculate the above integral in general, but it may be evaluated in the squeezed limit, say $k_3 \ll k_1 = k_2 \equiv k$. In this limit, the above reduces to

$$B^{\rm sq}_{\delta\chi^2}(k) \equiv B_{\delta\chi^2}(k,k,0) \simeq 8\int \widetilde{d^3q}\,|\delta\chi_q|^2|\delta\chi_{|\mathbf{k}-\mathbf{q}|}|^4\,. \tag{5.23}$$

In Appendix B, this integral is evaluated, and the result (given by Eq. (B14)) is

$$B^{\rm sq}_{\delta\chi^2}(k) \simeq \frac{\xi'^3}{k_c^3}\frac{H^4}{2\pi^2}P_{\delta\chi}(k) \simeq \left(\frac{\xi'}{\xi}\right)^3\frac{2H^2}{k_c^3}P_{\delta\chi^2}(k)\,, \tag{5.24}$$

where the second step follows from Eq. (B10) or (4.9), and ξ and ξ' are constants of order unity.

Another limiting case of interest is when the magnitudes of all the momenta are equal to each other, $k_1 = k_2 = k_3$, the so-called equilateral limit. Although we have no clue whatsoever to evaluate the bispectrum in this limit, it is plausible that the amplitude is at most of the same order as that in the squeezed limit, if not much smaller. So let us set

$$B^{\rm eq}_{\delta\chi^2}(k) = \xi^{\rm eq}\frac{2H^2}{k_c^3}P_{\delta\chi^2}(k)\,, \tag{5.25}$$

where $\xi^{\rm eq}$ is a non-dimensional factor supposedly of order unity.

C. Total bispectrum and f_{NL} parameter

It is customary to express the bispectrum of the curvature perturbation in terms of the non-Gaussianity parameter f_{NL} [53]. The standard definition of the non-Gaussianity parameter in Fourier space is [52]

$$\frac{6}{5}f_{NL}(k_1,k_2,k_3) = \frac{B_{\mathcal{R}}(k_1,k_2,k_3)}{[P_{\mathcal{R}}(k_1)P_{\mathcal{R}}(k_2)+\text{c.p.}]}\,. \tag{5.26}$$

In our case we may decompose it as

$$f_{NL} = f^{int}_{NL} + f^{dyn}_{NL} + f^{\phi}_{NL}\,, \tag{5.27}$$

where

$$\frac{6}{5}f^{int}_{NL} = \frac{B^{int}_{\mathcal{R}}(k_1,k_2,k_3)}{[P_{\mathcal{R}}(k_1)P_{\mathcal{R}}(k_2)+\text{c.p.}]} = -2\left(N_{,\chi^2}\right)^3\frac{B_{\delta\chi^2}(k_1,k_2,k_3)}{[P_{\mathcal{R}}(k_1)P_{\mathcal{R}}(k_2)+\text{c.p.}]}\,, \tag{5.28}$$

$$\frac{6}{5}f^{dyn}_{NL} = \frac{B^{dyn}_{\mathcal{R}}(k_1,k_2,k_3)}{[P_{\mathcal{R}}(k_1)P_{\mathcal{R}}(k_2)+\text{c.p.}]} = 3\frac{N_{,\chi^2\chi^2}}{(N_{,\chi^2})^2}\frac{\left[P^{wf}_{\mathcal{R}}(k_1)P^{wf}_{\mathcal{R}}(k_2)+\text{c.p.}\right]}{\left[P_{\mathcal{R}}(k_1)P_{\mathcal{R}}(k_2)+\text{c.p.}\right]} \tag{5.29}$$

$$\frac{6}{5}f^{\phi}_{NL} = \frac{B^{\phi}_{\mathcal{R}}(k_1,k_2,k_3)}{[P_{\mathcal{R}}(k_1)P_{\mathcal{R}}(k_2)+\text{c.p.}]} = \frac{1}{2}\frac{N_{,\phi\phi}}{(N_{,\phi})^2}\frac{\left[P^{\phi}_{\mathcal{R}}(k_1)P^{\phi}_{\mathcal{R}}(k_2)+\text{c.p.}\right]}{\left[P_{\mathcal{R}}(k_1)P_{\mathcal{R}}(k_2)+\text{c.p.}\right]}\,. \tag{5.30}$$

As noted before, the inflaton contribution f_{NL}^{ϕ} is known to be at most of the order of the slow-roll parameters, $f_{NL}^{\phi}=O(\epsilon,\eta)$ [54] hence can be safely neglected. So we focus on the contributions from the waterfall fields.

First let us consider f_{NL}^{dyn}. As clear from its form, it is non-negligible only when the amplitude of $P_{\mathcal{R}}^{wf}(k)$ is comparable to or greater than that of $P_{\mathcal{R}}^{\phi}(k)$, and this may happen only at and around the peak of the spectrum $k=k_{max}$. Then it is easy to see that f_{NL}^{dyn} is non-negligible only when all of k_1, k_2 and k_3 are approximately equal to k_{max}. Thus setting $k_1=k_2=k_3=k$ and assuming $P_{\mathcal{R}}^{wf}(k)$ dominates the spectrum, we find

$$\frac{6}{5}f_{NL}^{dyn}(k=k_{max})\simeq 3\frac{N_{,\chi^2\chi^2}}{\left(N_{,\chi^2}\right)^2}=-\frac{3\epsilon_\chi}{C\,\epsilon\,n_f^{1/2}}\,, \tag{5.31}$$

where we have used Eq. (C4) in Appendix C to eliminate $N_{,\chi^2}$ and $N_{,\chi^2\chi^2}$ from the intermediate expression. With $\epsilon_\chi\gg 1, C\ll 1$ and $n_f\sim 1$, we see that f_{NL}^{dyn} can become very large, centered around $k=k_{max}$. For example, for the parameters used in our numerical analysis, we have

$$\frac{6}{5}f_{NL}^{dyn}(k_{max})\simeq 7\times 10^4\,. \tag{5.32}$$

Next we consider f_{NL}^{int}. As clear from the form of $B_{\delta\chi^2}$ in Eq. (5.21), or its explicit evaluation, it remains finite in the squeezed limit, while the denominator of f_{NL}^{int} diverges since $P_{\mathcal{R}}^{\phi}$ is approximately proportional to k^{-3}. Therefore, f_{NL}^{int} is completely negligible in the squeezed limit. In contrast, the denominator is finite and of order k^{-6} in the equilateral limit. Hence, using Eq. (5.25), we obtain an estimate

$$\frac{6}{5}f_{NL}^{int}(k)\simeq \xi^{\rm eq}N_{,\chi^2}\,\frac{2H^2}{3k_c^3}\frac{P_{\mathcal{R}}^{wf}(k)}{P_{\mathcal{R}}^2(k)}=\xi^{\rm eq}N_{,\chi^2}\,\frac{2H^2}{3}\frac{k^3}{k_c^3}\frac{\mathcal{P}_{\mathcal{R}}^{wf}(k)}{\mathcal{P}_{\mathcal{R}}^2(k)}\,. \tag{5.33}$$

Again, this contribution to the non-Gaussianity is exponentially negligible except at around the peak of the waterfall field spectrum. Hence assuming $\mathcal{P}_{\mathcal{R}}^{wf}\simeq\mathcal{P}_{\mathcal{R}}$, and manipulating with the help of Eqs. (4.10), (4.11) and (C4), the above estimate gives

$$f_{NL}^{int}(k_{max})\sim \xi^{\rm eq}N_{,\chi^2}\,\frac{H^2k^3}{k_c^3}\frac{1}{\mathcal{P}_{\mathcal{R}}(k)}\sim \xi^{\rm eq}\epsilon_\chi^2 f_{NL}^{dyn}(k_{max})\,, \tag{5.34}$$

Depending on the value of the parameter $\xi^{\rm eq}$ of which we have no quantitative estimate, the intrinsic non-Gaussianity can be larger than the dynamical non-Gaussianity.

In any case, we conclude that the total non-Gaussianity parameter f_{NL} is at least as big as

$$f_{NL}(k_{max})=f_{NL}^{int}+f_{NL}^{dyn}\sim\frac{\epsilon_\chi}{C\epsilon\sqrt{n_f}}\,. \tag{5.35}$$

The width of this sharp feature in the bispectrum is the same as that of the spectrum, Eq. (2.38), ie, $\sigma(k)\sim 0.4k_{max}$.

VI. CONCLUSION AND DISCUSSIONS

In this paper we presented a dynamical mechanism to generate a sharp feature during inflation. The key role is played by the waterfall field χ which becomes tachyonic during inflation. We work in a region of the parameter space where the waterfall transition is fairly sharp, i.e., the duration of the transition is about one e-fold or so. Because of the coupling $g^2\phi^2\chi^2$ the phase transition induces a sharp but small change in the inflaton mass. In much of previous works in which sharp changes in the inflaton mass were studied, the focus was on the dynamics of the inflaton itself. In contrast, in our model a local feature is induced by non-trivial interactions between the waterfall and inflaton fields. In particular, the waterfall quantum fluctuations played the key role in determining the local feature.

Before the phase transition χ is very massive, so it has no classical evolution. It stays at its local minimum at $\chi=0$. When the inflation passes a critical value, χ becomes tachyonic and the waterfall transition commences. Then the squared fluctuation, $\langle\delta\chi^2\rangle$, starts to grow exponentially and the effective classical trajectory is determined by $\langle\delta\chi^2\rangle$ averaged over each Hubble horizon patch. The fluctuations from one horizon region to another, $\Delta\chi^2=\delta\chi^2-\langle\delta\chi^2\rangle$, determines the fluctuation around the classical trajectory.

We calculated the power spectrum of $\Delta\chi^2$ which is found to have a peak near the comoving scale k_c that crosses the horizon at the onset of transition, $k=k_{max}\sim k_c$. This in turn induces the curvature perturbation which shows a peak near $k = k_{max}$. The ratio of thus induced curvature perturbation to the conventional curvature perturbation from the inflaton field depends on the model parameters as given in Eq. (4.12). For reasonable values of the parameters, we find this ratio can become of order unity or even larger than unity.

This local feature we found may be used to explain the glitches found in the observed CMB angular power spectrum. One may also consider many waterfall fields coupled to the inflaton to produce a series of waterfall phase transitions and induce multiple local features in the curvature perturbation. It would be interesting to study numerically the effect of single or multiple local features in our model and compare it with CMB data.

Due to intrinsic non-Gaussian nature of $\delta\chi^2$ distribution one expects to see large spiky non-Gaussianities [55] when $\mathcal{P}_{\mathcal{R}}^{wf}(k_{max})$ becomes comparable to $\mathcal{P}_{\mathcal{R}}^{\phi}$. We have shown that f_{NL} has both intrinsic and dynamical contributions. The intrinsic contributions originates from $\delta\chi^2$ three-point function while the dynamical part comes from the non-linear dynamics of the waterfall field. It is shown that $f_{NL}(k_{max}) \sim \epsilon_\chi/\epsilon C$, in which ϵ_χ measures the sharpness of the waterfall phase transition. As a result, the sharper is the phase transition the larger is f_{NL}. As in the case of power spectrum, the bispectrum is highly peaked at $k \simeq k_{max}$. It would be very interesting to investigate the observational consequences of these spiky non-Gaussianities.

Acknowledgement

We would like to thank R. Allahverdi, X. Chen, E. Lim, K. Malik, S. Movahed, D. Mulryne and R. Tavakol for useful discussions and comments. A.A.A. would like to thank “Bonyad Nokhbegan Iran” for partial support. This work was supported in part by MEXT Grant-in-Aid for the global COE program at Kyoto University, ”The Next Generation of Physics, Spun from Universality and Emergence,” and by JSPS Grant-in-Aid for Scientific Research (A) No. 21244033.

Appendix A: Variance of waterfall field quantum fluctuations

Here we calculate $\langle\delta\chi^2(n)\rangle$ in some details. As discussed in the text, we must consider this as part of the classical background after it begins to evolve as a classical field,

$$\sqrt{\langle\delta\chi^2(n)\rangle} \propto \exp\left[\frac{2}{3}\epsilon_\chi n^{3/2}\right] . \tag{A1}$$

Then it is convenient to define $\langle\delta\chi^2(0)\rangle$ not by its actual value at $n = 0$, but the value it would take if it evolved classically from the beginning. That is, for modes that become tachyonic by the end of the waterfall transition $n = n_f$, we define

$$\langle\delta\chi^2(0)\rangle \equiv \langle\delta\chi^2(n_f)\rangle \exp\left[-\frac{4}{3}\epsilon_\chi n_f^{3/2}\right] . \tag{A2}$$

As mentioned in the text, we divide it into small scale and large scale parts, denoted by subscript S and L, respectively,

$$\langle\delta\chi^2(0)\rangle = \langle\delta\chi^2(0)\rangle_S + \langle\delta\chi^2(0)\rangle_L . \tag{A3}$$

As shown in [32], for the large scale part we have

$$\langle\delta\chi^2(0)\rangle_L = \frac{H^2}{4\pi^2\epsilon_\chi} . \tag{A4}$$

As for the contribution of small scale modes, as we show below, it was somewhat over-estimated in the previous literature. A more accurate result is obtained as follows.

As discussed around Eq. (2.29) in the text, we approximately have

$$\delta\chi_k^S(n) = \frac{H}{\sqrt{2k}\,k_c} e^{-n_t} \exp\left[\frac{2}{3}\epsilon_\chi (n^{3/2} - n_t^{3/2})\right] ; \quad n > n_t(k) . \tag{A5}$$

Literally speaking, however, the above does not reproduce the correct behavior when $n - n_t \ll 1$. At this stage, it behaves as

$$\delta\bar{\chi}_k^S(n) = \frac{H}{\sqrt{2k}\,k_c} e^{-n_t} \exp\left[\frac{2}{3}\epsilon_\chi (n - n_t)^{3/2}\right] . \tag{A6}$$

If we simply extrapolate this to $n = n_f$, we obtain

$$\delta\bar{\chi}_k^S(n_f) = \frac{H}{\sqrt{2k}\,k_c} e^{-n_t} \exp\left[\frac{2}{3}\epsilon_\chi (n_f - n_t)^{3/2}\right] , \tag{A7}$$

instead of the one that follows from the approximate formula (A5),

$$\delta\chi_k^S(n_f) = \frac{H}{\sqrt{2k}\,k_c} e^{-n_t} \exp\left[\frac{2}{3}\epsilon_\chi (n_f^{3/2} - n_t^{3/2})\right] . \tag{A8}$$

Then the formula (A7) gives an estimate of $\delta\chi_k^S(0)$ as

$$\begin{aligned} \delta\bar{\chi}_k^S(0) &= \frac{H}{\sqrt{2k}\,k_c} e^{-n_t} \exp\left[\frac{2}{3}\epsilon_\chi (n_f - n_t)^{3/2} - \epsilon_\chi n_f^{3/2}\right] \\ &= \delta\chi_k^S(0) \exp\left[\frac{2}{3}\epsilon_\chi (n_f - n_t)^{3/2} - \epsilon_\chi (n_f^{3/2} - n_t^{3/2})\right] , \end{aligned} \tag{A9}$$

where $\delta\chi_k^S(0)$ is estimated by using Eq. (A5). We easily see that $\delta\bar{\chi}_k^S(0) \leq \delta\chi_k^S(0)$. Thus one would expect that using $\delta\bar{\chi}_k^S(0)$ would give a slight underestimate, while using $\delta\chi_k^S(0)$ would give a slight overestimate.

Let us first estimate $\langle\delta\chi^2(0)\rangle_S$ by using $\delta\chi_k^S(0)$. Using Eq. (2.26), we find

$$\langle\delta\chi^2(0)\rangle_S = \frac{\epsilon_\chi^2 H^2}{4\pi^2} \int_{n_t=0}^{n_f} dn_t\,(n_t + \frac{1}{2}) e^{-4/3\epsilon_\chi n_t^{3/2}} . \tag{A10}$$

The exponential dependence of the integrand introduces a natural cut-off at $n_{cut} \sim \epsilon_\chi^{-2/3}$. Hence one can neglect n_t with respect to 1/2 in the integrand, and extend the integral range to infinity to obtain

$$\langle\delta\chi^2(0)\rangle_S \simeq \frac{\epsilon_\chi^2 H^2}{8\pi^2} \int_{n_t=0}^{\infty} dn_t\, e^{-4/3\epsilon_\chi n_t^{3/2}} = \frac{\epsilon_\chi^2 H^2}{8\pi^2} \frac{\Gamma\left(\frac{2}{3}\right)}{6^{1/3}\epsilon_\chi^{2/3}} \simeq 0.75 \frac{\epsilon_\chi^{4/3} H^2}{8\pi^2} . \tag{A11}$$

This gives a slightly overestimate of the true $\langle\delta\chi^2(0)\rangle_S$.

Now let us consider using $\delta\bar{\chi}_k^S(0)$. Instead of the integral (A10), we have

$$\langle\delta\bar{\chi}^2(0)\rangle_S = \frac{\epsilon_\chi^2 H^2}{4\pi^2} \int_{n_t=0}^{n_f} dn_t\,(n_t + \frac{1}{2}) \exp\left[\frac{4}{3}\epsilon_\chi n_f^{3/2}\left(\left(1 - \frac{n_t}{n_f}\right)^{3/2} - 1\right)\right] . \tag{A12}$$

Again, similar to the previous case, the integral is dominated by the integrand at $n_t/n_f \ll 1$. Then expanding the exponent in n_t/n_f, we may approximate it by

$$\langle\delta\bar{\chi}^2(0)\rangle_S \simeq \frac{\epsilon_\chi^2 H^2}{8\pi^2} \int_{n_t=0}^{n_f} dn_t \exp\left[-2\epsilon_\chi n_f^{1/2} n_t\right] \simeq \frac{\epsilon_\chi^2 H^2}{8\pi^2} \frac{1}{2\epsilon_\chi n_f^{1/2}} = \frac{\epsilon_\chi H^2}{16\pi^2 n_f^{1/2}} . \tag{A13}$$

This result is by a factor $\epsilon_\chi^{1/3} n_f^{-1/2}$ smaller than the estimate (A11). For a typical value of ϵ_χ and n_f, say $\epsilon_\chi \sim 10$ and $n_f \sim 0.5$, however, this factor is $\epsilon_\chi^{1/3} n_f^{-1/2} \sim 1.5$. So qualitatively there is not much difference between the two estimates.

To summarize, we conclude that the dominant contribution to the variance of the small scale waterfall field quantum fluctuations comes from the modes around $\epsilon_\chi^{-1} n_f^{-1/2} \lesssim n \lesssim \epsilon_\chi^{-2/3}$, and given by somewhere between Eqs. (A11) and (A13). Comparing these with Eq. (A4), we readily see that the dominant contribution to the variance of the waterfall field quantum fluctuations comes from the small scale modes,

$$\langle\delta\chi^2(0)\rangle = \langle\delta\chi^2(0)\rangle_S + \langle\delta\chi^2(0)\rangle_L \simeq \langle\delta\chi^2(0)\rangle_S . \tag{A14}$$

Since there is not much difference between Eqs. (A11) and (A13), for definiteness we use Eq. (A11) in the text.

Appendix B: Correlation functions of square of waterfall field quanta $\mathcal{P}\delta\chi^2$

This appendix is devoted to find a good approximation for the correlation functions of the $\delta\chi^2$ appearing in the power spectrum and bispectrum analysis, Eqs. (4.8) and (5.22).

First, we work out the following convolution integral which is necessary is calculations of power spectrum of the waterfall field

$$\Big\langle \left(\delta\chi^2\right)_k \left(\delta\chi^2\right)_q \Big\rangle \;=\; 2\int \frac{d^3q}{(2\pi)^3}|\delta\chi_{|\mathbf{k}-\mathbf{q}|}|^2|\delta\chi_q|^2 \;(2\pi)^3\delta^3(\mathbf{k}+\mathbf{q}). \tag{B1}$$

The above integral can be divided into the radial and angular parts as follows

$$2\int \frac{d^3q}{(2\pi)^3}|\delta\chi_{|\mathbf{k}-\mathbf{q}|}|^2|\delta\chi_q|^2 = \int dn_q \mathcal{P}_{\delta\chi}(q)\int d(-\cos\theta)|\delta\chi_{|\mathbf{k}-\mathbf{q}|}|^2\,. \tag{B2}$$

The above integral can not be calculated analytically but can be estimated as follows. First, note that as the power spectrum of waterfall field $\mathcal{P}_{\delta\chi}$ is highly peaked around $k = k_{max}$ so one can expect that the peak of curvature perturbation $\mathcal{P}_{\mathcal{R}} \sim \mathcal{P}_{\delta\chi^2}$ also take place near $k_{max} \gg k_c$. This assumption will be checked in the following. The other main point is that Eq. (2.33) shows that $|\delta\chi_{|\mathbf{k}-\mathbf{q}|}|^2$ is constant value $\frac{H_0^2}{2k_c^3}$ for $|\mathbf{k}-\mathbf{q}| < k_c$ and exponentially decay for $|\mathbf{k}-\mathbf{q}| > k_c$. As a result one can conclude that the second integral in Eq. (B2) is negligible except for

$$|\mathbf{k}-\mathbf{q}| \lesssim \xi k_c \tag{B3}$$

in which the numerical factor ξ can be estimated from Eq. (2.30). To find an estimate of ξ it is natural to estimate the width of integration, Δk, the point at which $P_{\delta\chi}$ decreased by a factor $1/e$ from its value at $k = k_c$, $P_{\delta\chi}(k_c) = H_0^2/(2k^3)$. So by using Eq. (2.30) and noting that for $k \sim k_c$, $n_t(k) \ll n_*(k)$, one has

$$\xi \simeq e. \tag{B4}$$

In order to satisfy condition (B3) one can simply find that the amplitude of integral momentum q should be near k and at the same time the angle between $\mathbf{k}$ and $\mathbf{q}$, denoted by θ, should be near zero. By defining

$$q = k + \Delta q, \qquad \Delta q < k, \qquad \text{and} \qquad \theta = 0 + \Delta\theta \tag{B5}$$

one can find that the condition

$$|\mathbf{k}-\mathbf{q}|^2 \lesssim \xi^2 k_c^2 \tag{B6}$$

results in

$$\Delta q \lesssim \xi k_c \qquad \longrightarrow \qquad \Delta n_q \lesssim \frac{\xi k_c}{k} \tag{B7}$$

$$\Delta(-\cos\theta) \quad = \quad \frac{\xi^2\, k_c^2}{2k^2} \tag{B8}$$

With these approximations the integral Eq. (B2) can be estimated for $k \gg k_c$ as

$$\begin{aligned} 2\int \frac{d^3q}{(2\pi)^3}|\delta\chi_{|\mathbf{k}-\mathbf{q}|}|^2|\delta\chi_q|^2 \;&=\; 2\int dn_q\; d(-\cos\theta)|\delta\chi_{|\mathbf{k}-\mathbf{q}|}|^2\mathcal{P}_{|\delta\chi|}(q) \\ &\simeq\; \Delta n_q\, \Delta(-\cos\theta)\frac{H_0^2}{2k_c^3}\mathcal{P}_{\delta\chi}(k) \\ &=\; \frac{\xi^3\, H_0^2}{2k^3}\mathcal{P}_{\delta\chi}(k) \end{aligned} \tag{B9}$$

Finally one can find the following good approximate for $\mathcal{P}_{\delta\chi^2}$ in terms of $\mathcal{P}_{\delta\chi}$

$$\mathcal{P}_{\delta\chi^2}(k) \simeq \frac{\xi^3\, H_0^2}{4\pi^2}\,\mathcal{P}_{\delta\chi}(k). \tag{B10}$$

Similarly, we present an approximation for the three point correlation function of $\delta\chi^2$ in the squeezed form

$$\langle\, \left(\delta\chi^2\right)_{\mathbf{k}_1} \left(\delta\chi^2\right)_{\mathbf{k}_2} \left(\delta\chi^2\right)_{\mathbf{k}_3} \rangle_{\rm sq} \simeq 8\,\delta^3(\mathbf{k}_1+\mathbf{k}_2+\mathbf{k}_3)\int d^3q|\delta\chi_q|^2|\delta\chi_{|\mathbf{k}-\mathbf{q}|}|^4\,. \tag{B11}$$

One can approximate the above integral in the same fashion as we did above for the two point correlation function

$$\left\langle \left(\delta\chi^2\right)_{\mathbf{k}_1} \left(\delta\chi^2\right)_{\mathbf{k}_2} \left(\delta\chi^2\right)_{\mathbf{k}_3} \right\rangle_{\rm sq} \simeq 8(2\pi)^3\delta^3(\mathbf{k}_1+\mathbf{k}_2+\mathbf{k}_3)\int dn_q \mathcal{P}_{\delta\chi}(q)\int d(-\cos\theta)|\delta\chi_{|\mathbf{k}-\mathbf{q}|}|^4 \tag{B12}$$

By using the above relation, one finds

$$\begin{aligned} B^{\rm sq}_{\delta\chi^2} &= 8\int dn_q \mathcal{P}_{\delta\chi}(q)\int d(-\cos\theta)|\delta\chi_{|\mathbf{k}-\mathbf{q}|}|^4 \\ &\simeq 8\Delta n_q\,\Delta(-\cos\theta)\frac{H_0^4}{4k_c^6}\mathcal{P}_{\delta\chi}(k) \\ &= \frac{\xi'^3\,H_0^4}{k_c^3k^3}\mathcal{P}_{\delta\chi}(k)\,, \end{aligned} \tag{B13}$$

in which the numerical factor ξ', similarly defined as ξ, is obtained to be $\xi'\simeq\sqrt{e}$. Finally one has

$$B^{\rm sq}_{\delta\chi^2}(k) \simeq \frac{\xi'^3}{k_c^3}\frac{H_0^4}{2\pi^2}P_{\delta\chi}(k)\,. \tag{B14}$$

Appendix C: $\delta\mathcal{N}$ up to order $\Delta\chi^4$

In order to find $\delta\mathcal{N}$ up to order $\Delta\chi^4$ it is enough to extend Eq. (3.14) to next order in $\delta\chi^2$, which reads

$$\frac{\Delta\chi^2(n)}{\langle\delta\chi^2(n)\rangle} - \frac{1}{2}\frac{\Delta\chi^4(n)}{\langle\delta\chi^2(n)\rangle^2} = \frac{\delta\chi^2_{min}(n_f)}{\chi^2_{min}(n_f)} + 2f'(n)\delta n - 2f'(n_f)\delta n_f\,. \tag{C1}$$

This modifies $\delta\mathcal{N}$ in Eq. (3.18) to

$$\begin{aligned} \delta\mathcal{N} &= \left(\frac{\Delta\chi^2(n)}{\langle\delta\chi^2(n)\rangle} - \frac{1}{2}\frac{\Delta\chi^4(n)}{\langle\chi^2(n)\rangle^2}\right)\left[\frac{\partial n}{\partial n_f}\frac{1}{-2f'(n_f)+n_f^{-1}}\right] \\ &\quad + \frac{\phi\,\delta\phi(n)}{2M_P^2}\left[1+\frac{C}{2}+C\epsilon n + \frac{2f'(n)}{-2f'(n_f)+n_f^{-1}}\frac{\partial n}{\partial n_f}\right]\,. \end{aligned} \tag{C2}$$

For a sharp transition, $n_f \lesssim 1$, the above expression reduces to

$$\delta\mathcal{N} = -\frac{C\epsilon n_f}{f'(n_f)}\left(\frac{\Delta\chi^2(n)}{\langle\delta\chi^2(n)\rangle} - \frac{1}{2}\frac{\Delta\chi^4(n)}{\langle\chi^2(n)\rangle^2}\right) + \left[1+\frac{C}{2}+C\epsilon(n-2n_f)\right]\frac{\phi\delta\phi}{2M_P^2}\,. \tag{C3}$$

From the above, we find the relation between $N_{,\chi^2}$ and $N_{,\chi^2\chi^2}$ as

$$N_{,\chi^2} = -\langle\delta\chi^2(0)\rangle N_{,\chi^2,\chi^2} = \frac{-C\,\epsilon\,n_f}{f'(n_f)}\frac{1}{\langle\delta\chi^2(0)\rangle} = -\frac{C\,\epsilon}{n_f^{1/2}\epsilon_\chi}\frac{1}{\langle\delta\chi^2(0)\rangle}\,, \tag{C4}$$

where the second equality follows from the fact that $f'(n) = \epsilon_\chi n^{1/2}$.

---

[1] E. Komatsu *et al.*, "Seven-Year Wilkinson Microwave Anisotropy Probe (WMAP) Observations: Cosmological Interpretation," arXiv:1001.4538 [astro-ph.CO].

[2] A. A. Starobinsky, "Spectrum of adiabatic perturbations in the universe when there are singularities in the inflation potential," JETP Lett. **55**, 489 (1992) [Pisma Zh. Eksp. Teor. Fiz. **55**, 477 (1992)].

[3] S. M. Leach, M. Sasaki, D. Wands and A. R. Liddle, Phys. Rev. D **64**, 023512 (2001) [astro-ph/0101406].

[4] J. A. Adams, B. Cresswell, R. Easther, "Inflationary perturbations from a potential with a step," Phys. Rev. **D64**, 123514 (2001). [astro-ph/0102236].

[5] J. -O. Gong, "Breaking scale invariance from a singular inflaton potential," JCAP **0507**, 015 (2005) [astro-ph/0504383].

[6] M. Joy, V. Sahni, A. A. Starobinsky, “A New Universal Local Feature in the Inflationary Perturbation Spectrum,” Phys. Rev. **D77**, 023514 (2008). [arXiv:0711.1585 [astro-ph]].

[7] X. Chen, R. Easther and E. A. Lim, “Large Non-Gaussianities in Single Field Inflation,” JCAP **0706**, 023 (2007) [astro-ph/0611645].

[8] X. Chen, R. Easther and E. A. Lim, “Generation and Characterization of Large Non-Gaussianities in Single Field Inflation,” JCAP **0804**, 010 (2008) [arXiv:0801.3295 [astro-ph]].

[9] X. Chen, “Primordial Features as Evidence for Inflation,” JCAP **1201**, 038 (2012) [arXiv:1104.1323 [hep-th]].

[10] X. Chen, “Fingerprints of Primordial Universe Paradigms as Features in Density Perturbations,” Phys. Lett. B **706**, 111 (2011) [arXiv:1106.1635 [astro-ph.CO]].

[11] S. Hotchkiss and S. Sarkar, “Non-Gaussianity from violation of slow-roll in multiple inflation,” JCAP **1005**, 024 (2010) [arXiv:0910.3373 [astro-ph.CO]].

[12] F. Arroja, A. E. Romano and M. Sasaki, “Large and strong scale dependent bispectrum in single field inflation from a sharp feature in the mass,” Phys. Rev. D **84**, 123503 (2011) [arXiv:1106.5384 [astro-ph.CO]].

[13] P. Adshead, C. Dvorkin, W. Hu and E. A. Lim, “Non-Gaussianity from Step Features in the Inflationary Potential,” Phys. Rev. D **85**, 023531 (2012) [arXiv:1110.3050 [astro-ph.CO]].

[14] A. E. Romano and M. Sasaki, Phys. Rev. D **78**, 103522 (2008) [arXiv:0809.5142 [gr-qc]].

[15] D. Battefeld, T. Battefeld, H. Firouzjahi and N. Khosravi, “Brane Annihilations during Inflation,” JCAP **1007**, 009 (2010) [arXiv:1004.1417 [hep-th]].

[16] H. Firouzjahi and S. Khoeini-Moghaddam, “Fields Annihilation and Particles Creation in DBI inflation,” JCAP **1102**, 012 (2011) [arXiv:1011.4500 [hep-th]].

[17] D. Battefeld, T. Battefeld, J. T. Giblin, Jr. and E. K. Pease, “Observable Signatures of Inflaton Decays,” JCAP **1102**, 024 (2011) [arXiv:1012.1372 [astro-ph.CO]].

[18] N. Barnaby and Z. Huang, “Particle Production During Inflation: Observational Constraints and Signatures,” Phys. Rev. D **80**, 126018 (2009) [arXiv:0909.0751 [astro-ph.CO]].

[19] N. Barnaby, “On Features and Nongaussianity from Inflationary Particle Production,” Phys. Rev. D **82**, 106009 (2010) [arXiv:1006.4615 [astro-ph.CO]]; N. Barnaby, “Nongaussianity from Particle Production During Inflation,” Adv. Astron. **2010**, 156180 (2010) [arXiv:1010.5507 [astro-ph.CO]].

[20] T. Biswas, A. Mazumdar and A. Shafieloo, “Wiggles in the cosmic microwave background radiation: echoes from non-singular cyclic-inflation,” Phys. Rev. D **82**, 123517 (2010) [arXiv:1003.3206 [hep-th]].

[21] E. Silverstein and A. Westphal, “Monodromy in the CMB: Gravity Waves and String Inflation,” Phys. Rev. D **78**, 106003 (2008) [arXiv:0803.3085 [hep-th]].

[22] R. Flauger, L. McAllister, E. Pajer, A. Westphal and G. Xu, “Oscillations in the CMB from Axion Monodromy Inflation,” JCAP **1006**, 009 (2010) [arXiv:0907.2916 [hep-th]].

[23] R. Flauger and E. Pajer, “Resonant Non-Gaussianity,” JCAP **1101**, 017 (2011) [arXiv:1002.0833 [hep-th]].

[24] R. Bean, X. Chen, G. Hailu, S. -H. H. Tye and J. Xu, “Duality Cascade in Brane Inflation,” JCAP **0803**, 026 (2008) [arXiv:0802.0491 [hep-th]].

[25] A. D. Linde, “Hybrid inflation,” Phys. Rev. D **49**, 748 (1994) [arXiv:astro-ph/9307002].

[26] A. R. Liddle, D. H. Lyth, E. D. Stewart and D. Wands, “False vacuum inflation with Einstein gravity,” Phys. Rev. D **49**, 6410 (1994) [arXiv:astro-ph/9401011].

[27] D. Wands, K. A. Malik, D. H. Lyth *et al.*, “A New approach to the evolution of cosmological perturbations on large scales,” Phys. Rev. **D62**, 043527 (2000). [astro-ph/0003278].

[28] D. H. Lyth, “Issues concerning the waterfall of hybrid inflation,” arXiv:1005.2461 [astro-ph.CO].

[29] A. A. Abolhasani, H. Firouzjahi, “No Large Scale Curvature Perturbations during Waterfall of Hybrid Inflation,” Phys. Rev. **D83**, 063513 (2011). [arXiv:1005.2934 [hep-th]].

[30] J. Fonseca, M. Sasaki, D. Wands, “Large-scale Perturbations from the Waterfall Field in Hybrid Inflation,” JCAP **1009**, 012 (2010). [arXiv:1005.4053 [astro-ph.CO]].

[31] A. A. Abolhasani, H. Firouzjahi, M. Sasaki, “Curvature perturbation and waterfall dynamics in hybrid inflation,” [arXiv:1106.6315 [astro-ph.CO]].

[32] J. -O. Gong, M. Sasaki, “Waterfall field in hybrid inflation and curvature perturbation,” JCAP **1103**, 028 (2011). [arXiv:1010.3405 [astro-ph.CO]].

[33] D. H. Lyth, “The hybrid inflation waterfall and the primordial curvature perturbation,” arXiv:1201.4312 [astro-ph.CO].

[34] D. H. Lyth, “Primordial black hole formation and hybrid inflation,” arXiv:1107.1681 [astro-ph.CO].

[35] L. P. Levasseur, G. Laporte, R. Brandenberger, “Analytical Study of Mode Coupling in Hybrid Inflation,” Phys. Rev. **D82**, 123524 (2010). [arXiv:1004.1425 [hep-th]].

[36] N. Barnaby and J. M. Cline, “Nongaussianity from Tachyonic Preheating in Hybrid Inflation,” Phys. Rev. D **75**, 086004 (2007) [arXiv:astro-ph/0611750];
N. Barnaby and J. M. Cline, “Nongaussian and nonscale-invariant perturbations from tachyonic preheating in hybrid inflation,” Phys. Rev. D **73**, 106012 (2006) [arXiv:astro-ph/0601481].

[37] A. Mazumdar, J. Rocher, “Particle physics models of inflation and curvaton scenarios,” Phys. Rept. **497**, 85-215 (2011). [arXiv:1001.0993 [hep-ph]].

[38] K. Enqvist, A. Jokinen, A. Mazumdar, T. Multamaki and A. Vaihkonen, “Non-Gaussianity from Preheating,” Phys. Rev. Lett. **94**, 161301 (2005) [arXiv:astro-ph/0411394];
K. Enqvist, A. Jokinen, A. Mazumdar, T. Multamaki and A. Vaihkonen, “Non-gaussianity from instant and tachyonic preheating,” JCAP **0503**, 010 (2005) [arXiv:hep-ph/0501076].

[39] K. Enqvist and A. Vaihkonen, “Non-Gaussian perturbations in hybrid inflation,” JCAP **0409**, 006 (2004) [arXiv:hep-ph/0405103].

[40] L. Randall, M. Soljacic, A. H. Guth, “Supernatural inflation: Inflation from supersymmetry with no (very) small parameters,” Nucl. Phys. **B472**, 377-408 (1996). [hep-ph/9512439].

[41] J. Garcia-Bellido, A. D. Linde, D. Wands, “Density perturbations and black hole formation in hybrid inflation,” Phys. Rev. **D54**, 6040-6058 (1996). [astro-ph/9605094].

[42] S. Clesse, “Hybrid inflation along waterfall trajectories,” Phys. Rev. D **83**, 063518 (2011) [arXiv:1006.4522 [gr-qc]].

[43] J. Martin and V. Vennin, “Stochastic Effects in Hybrid Inflation,” Phys. Rev. D **85**, 043525 (2012) [arXiv:1110.2070 [astro-ph.CO]].

[44] D. Mulryne, S. Orani and A. Rajantie, “Non-Gaussianity from the hybrid potential,” Phys. Rev. D **84**, 123527 (2011) [arXiv:1107.4739 [hep-th]].

[45] A. Avgoustidis, S. Cremonini, A. -C. Davis, R. H. Ribeiro, K. Turzynski and S. Watson, “The Importance of Slow-roll Corrections During Multi-field Inflation,” JCAP **1202**, 038 (2012) [arXiv:1110.4081 [astro-ph.CO]].

[46] H. Kodama, K. Kohri and K. Nakayama, “On the waterfall behavior in hybrid inflation,” Prog. Theor. Phys. **126**, 331 (2011) [arXiv:1102.5612 [astro-ph.CO]].

[47] A. A. Abolhasani, H. Firouzjahi, M. H. Namjoo, “Curvature Perturbations and non-Gaussianities from Waterfall Phase Transition during Inflation,” [arXiv:1010.6292 [astro-ph.CO]].

[48] E. Bugaev and P. Klimai, “Curvature perturbation spectra from waterfall transition, black hole constraints and non-Gaussianity,” JCAP **1111**, 028 (2011) [arXiv:1107.3754 [astro-ph.CO]].

[49] E. Bugaev and P. Klimai, “Formation of primordial black holes from non-Gaussian perturbations produced in a waterfall transition,” arXiv:1112.5601 [astro-ph.CO].

[50] M. Sasaki, E. D. Stewart, “A General analytic formula for the spectral index of the density perturbations produced during inflation,” Prog. Theor. Phys. **95**, 71-78 (1996). [astro-ph/9507001].

[51] M. Sasaki and T. Tanaka, “Superhorizon scale dynamics of multiscalar inflation,” Prog. Theor. Phys. **99**, 763 (1998) [gr-qc/9801017].

[52] D. H. Lyth and A. R. Liddle, *Primordial Density Perturbation* (Cambridge University Press, 2009).

[53] E. Komatsu and D. N. Spergel, “Acoustic signatures in the primary microwave background bispectrum,” Phys. Rev. D **63**, 063002 (2001) [astro-ph/0005036].

[54] J. M. Maldacena, “Non-Gaussian features of primordial fluctuations in single field inflationary models,” JHEP **0305**, 013 (2003) [astro-ph/0210603].

[55] J. R. Bond, A. V. Frolov, Z. Huang and L. Kofman, “Non-Gaussian Spikes from Chaotic Billiards in Inflation Preheating,” Phys. Rev. Lett. **103**, 071301 (2009) [arXiv:0903.3407 [astro-ph.CO]].